The Plant Cell, Vol. 24: 3278–3295, August 2012, www.plantcell.org 

# SKIP Is a Component of the Spliceosome Linking Alternative Splicing and the Circadian Clock in *Arabidopsis*[W]

**Xiaoxue Wang,[a,1,2] Fangming Wu,[a,b,c,1] Qiguang Xie,[d,1] Huamei Wang,[a] Ying Wang,[e] Yanling Yue,[a] Ondrej Gahura,[f] Shuangshuang Ma,[a,c] Lei Liu,[a,c] Ying Cao,[a,c] Yuling Jiao,[e] Frantisek Puta,[f] C. Robertson McClung,[d] Xiaodong Xu,[c] and Ligeng Ma[a,c,g,3,4]**

[a] National Institute of Biological Sciences, Beijing 102206, China
[b] College of Life Sciences, Beijing Normal University, Beijing 100875, China
[c] Hebei Key Laboratory of Molecular Cell Biology, College of Biological Sciences, Hebei Normal University, Shijiazhuang 050016, Hebei, China
[d] Department of Biological Sciences, Dartmouth College, Hanover, New Hampshire 03755-3576
[e] Institute of Genetics and Developmental Biology, Chinese Academy of Science, Beijing 100101, China
[f] Department of Cell Biology, Faculty of Science, Charles University in Prague, Prague 128 00, Czech Republic
[g] College of Biological Sciences, Capital Normal University, Beijing 100048, China

**Circadian clocks generate endogenous rhythms in most organisms from cyanobacteria to humans and facilitate entrainment to environmental diurnal cycles, thus conferring a fitness advantage. Both transcriptional and posttranslational mechanisms are prominent in the basic network architecture of circadian systems. Posttranscriptional regulation, including mRNA processing, is emerging as a critical step for clock function. However, little is known about the molecular mechanisms linking RNA metabolism to the circadian clock network. Here, we report that a conserved SNW/Ski-interacting protein (SKIP) domain protein, SKIP, a splicing factor and component of the spliceosome, is involved in posttranscriptional regulation of circadian clock genes in *Arabidopsis thaliana*. Mutation in *SKIP* lengthens the circadian period in a temperature-sensitive manner and affects light input and the sensitivity of the clock to light resetting. SKIP physically interacts with the spliceosomal splicing factor Ser/Arg-rich protein45 and associates with the pre-mRNA of clock genes, such as *PSEUDORESPONSE REGULATOR7* (*PRR7*) and *PRR9*, and is necessary for the regulation of their alternative splicing and mRNA maturation. Genome-wide investigations reveal that SKIP functions in regulating alternative splicing of many genes, presumably through modulating recognition or cleavage of 5′ and 3′ splice donor and acceptor sites. Our study addresses a fundamental question on how the mRNA splicing machinery contributes to circadian clock function at a posttranscriptional level.**

## INTRODUCTION

The circadian clock plays critical role in diverse aspects of plant growth and development and in coordination of the biological activities with daily environmental cycles (McClung, 2006; Harmer, 2009). Circadian clocks are composed of negative feedback loops, although the specific core clock components recruited to form circadian oscillators vary among taxa (Bell-Pedersen et al., 2005; Wijnen and Young, 2006; McClung and Gutiérrez, 2010; Zhang and Kay, 2010).

In *Arabidopsis thaliana*, as in most other eukaryotes studied to date, a circadian clock includes multiple interlocked feedback loops. The initially described central loop is based on reciprocal regulation between *CIRCADIAN CLOCK ASSOCIATED1* (*CCA1*)/*LATE ELONGATED HYPOCOTYL* (*LHY*) and *TIMING OF CAB EXPRESSION1* (*TOC1*) (Harmer, 2009). In this loop, *CCA1* and *LHY* repress *TOC1* expression through direct promoter binding. Similarly, *TOC1* binds directly to specific regions of the *CCA1* and *LHY* promoters as a transcriptional repressor (Harmer, 2009; Gendron et al., 2012; Huang et al., 2012; Pokhilko et al., 2012). This central loop integrates with two other morning and evening loops to establish the basic architecture of the plant circadian clock. The expression of *PSEUDORESPONSE REGULATOR7* (*PRR7*) and *PRR9*, two homologs of TOC1, is directly activated by CCA1 and LHY, and in turn PRR7 and PRR9 suppress the expression of *CCA1* and *LHY* in the morning loop. Mutations in *PRR7* and *PRR9* lead to long circadian period, whereas mutations in *CCA1*, *LHY*, and *TOC1* shorten circadian period (Harmer, 2009).

TOC1, PRR5, GIGANTEA (GI), LUX ARRHYTHMO (LUX; also called PHYTOCLOCK1), and possibly other circadian components play essential roles in the night-specific loop (Hazen et al., 2005; Onai and Ishiura, 2005; Más and Yanovsky, 2009; Harmer,

[1] These authors contributed equally to this work.
[2] Current address: Rice Research Institute, College of Agronomy, Shenyang Agricultural University, Shenyang 110866, China.
[3] Current address: College of Biological Sciences, Capital Normal University, Beijing 100048, China.
[4] Address correspondence to ligeng.ma@mail.hebtu.edu.cn.
The authors responsible for distribution of materials integral to the findings presented in this article in accordance with the policy described in the Instructions for Authors (www.plantcell.org) are Ligeng Ma (ligeng.ma@mail.hebtu.edu.cn) and Xiaodong Xu (xiaodong.xu@mail.hebtu.edu.cn).
[W] Online version contains Web-only data.
www.plantcell.org/cgi/doi/10.1105/tpc.112.100081

2010; McClung and Gutiérrez, 2010; Nakamichi et al., 2010; Pruneda-Paz and Kay, 2010; Wang et al., 2010). LUX, in an evening complex with EARLY FLOWERING3 (ELF3) and ELF4, has been recently shown to link the evening and morning loops by negatively regulating *PRR9* expression via direct promoter binding (Helfer et al., 2011; Nusinow et al., 2011; Chow et al., 2012). Limiting light input, either by reducing fluence rate and abundance of photoreceptors, or blocking photoreceptor cascades slows the pace of the oscillator (Millar et al., 1995; Somers et al., 1998). Many other clock components, including REVEILLE8 (Farinas and Mas, 2011; Rawat et al., 2011), TIME FOR COFFEE (Hall et al., 2003; Ding et al., 2007), GI (Park et al., 1999; Tseng et al., 2004; Mizoguchi et al., 2005), and XAP5 CIRCADIAN TIMEKEEPER (Martin-Tryon and Harmer, 2008) have been identified, although how these contribute to clock function remains incompletely understood.

In addition, posttranslational regulatory mechanisms, including regulated protein modification by phosphorylation and proteasomal degradation, are also a theme seen in clocks of most taxa (Harms et al., 2004; Guo et al., 2009; Mehra et al., 2009). Proteasome-mediated degradation of TOC1 and its homolog PRR5 are triggered through interaction with the cytosolic F-box protein ZEITLUPE (ZTL) (Más et al., 2003; Kiba et al., 2007; Kim et al., 2007). Phosphorylation also regulates activity and abundance of clock components. Phosphorylation of CCA1, mediated at least in part by Casein Kinase2, is required for its normal function (Sugano et al., 1998; Daniel et al., 2004). TOC1 and each of the PRRs exhibit cycling levels of phosphorylation, although the responsible kinases are unknown (Fujiwara et al., 2008). Phosphorylation of PRR3 promotes its interaction with TOC1, which stabilizes TOC1 by sequestering it from ZTL (Para et al., 2007; Fujiwara et al., 2008). Interaction of PRR5 with TOC1 promotes the nuclear localization of TOC1, which is necessary for its function (Wang et al., 2010).

Pre-mRNA processing (5′ capping, splicing, and 3′ polyadenylation) is an essential step in eukaryotic gene expression that not only affects the mature mRNA level but is intimately interconnected with both transcription itself and downstream mRNA metabolic events including mRNA export and turnover (Moore and Proudfoot, 2009). Pre-mRNA splicing takes place within the spliceosome. Components of the splicing complex include several small nuclear ribonucleoproteins (snRNPs), numerous Ser/Arg-rich (SR) proteins, and other non-snRNP proteins. The SR proteins act as splicing factors in either constitutive or alternative splicing (Deckert et al., 2006; Behzadnia et al., 2007; Bessonov et al., 2008). The spliceosome is highly dynamic during splicing progression, guided by consensus sequences in the pre-mRNA to form sequential complexes (Wahl et al., 2009).

Splicing has been employed by plants to modulate gene expression and development (Lorković et al., 2000; Reddy, 2007). Alternative processing of the tobacco (*Nicotiana tabacum*) N gene and of the *Arabidopsis Flowering Time Control Locus A* pre-mRNA is an important regulatory stage in the control of disease resistance and of the floral transition (Dinesh-Kumar and Baker, 2000; Jordan et al., 2002; Macknight et al., 2002; Quesada et al., 2003). Dysfunction of the plant-specific SR45 protein leads to splicing deficiency and late flowering, as well as to abnormal leaf morphological defects (Ali et al., 2007; Tanabe et al., 2009; Zhang and Mount, 2009). Alternative splicing is also emerging as an important mechanism to regulate clock gene expression, including the *period* gene in *Drosophila melanogaster* (Cheng et al., 1998), the *frequency* gene in *Neurospora crassa* (Colot et al., 2005), and the *CCA1* gene in *Arabidopsis* (Filichkin et al., 2010). Recently, temperature-dependent alternative splicing has been shown to contribute to temperature compensation of the plant circadian clock (James et al., 2012). PROTEIN ARGININE METHYL TRANSFERASE5 (PRMT5) has been shown to contribute to circadian period determination in *Arabidopsis*, at least in part through the regulation of alternative splicing of *PRR9* (Hong et al., 2010; Sanchez et al., 2010). PRMT5, a type II protein Arg methyltransferase, methylates various non-histone substrates, such as heterogeneous nuclear ribonucleoproteins, snRNP, SmD1, D3, and LSm4, and reduced methylation of SmD1 and LSm4 is thought to elongate the circadian period of *prmt5* mutants (Deng et al., 2010; Sanchez et al., 2010).

In this work, we characterize a novel mutant with a defective (long) circadian period and show that the mutation disrupts the function of a gene encoding the *Arabidopsis* homolog of mammalian Ski-interacting protein (SKIP). Our studies reveal that in *Arabidopsis* SKIP is a component of a splicing complex and plays a pivotal role in pre-mRNA splicing of several circadian oscillator genes through direct pre-mRNA binding. Mutations of *SKIP* compromise splice site choice and, hence, alter genome-wide splicing patterns. Splicing defects in clock genes, including *PRR7* and *PRR9*, contribute to a lengthened period of the circadian clock. Our studies reveal a critical role for the SKIP splicing factor in the regulation of splicing and in the determination of circadian period.

## RESULTS

### Mutation of *EIP1* Confers Circadian Defects in *Arabidopsis*

To find new components in the floral transition pathway, we performed a genetic screen in a T-DNA–mutagenized background for early flowering mutants. From this, we isolated a recessive mutant that exhibits an early flowering phenotype under both long-day (LD) and short-day photoperiod conditions, which we have designated as *early flowering and insensitive to photoperiod1-1* (*eip1-1*) (see Supplemental Table 1 online). Because some mutants affecting circadian clock function exhibit a photoperiod-insensitive phenotype in terms of flowering, we tested *eip1-1* for altered rhythmicity and observed a lengthened (by ~2.4 h) period of circadian leaf movement in continuous white light (LL) (Figure 1A; see Supplemental Table 2 online). We then tested the expression of the circadian clock-controlled *LHCB1*1* (*CAB2*) gene, encoding a light-harvesting chlorophyll *a/b* binding protein, and observed a similar long period in *eip1-1* under LL (Figure 1B; see Supplemental Table 2 online). Thus, *EIP1* is necessary for circadian period determination of multiple circadian clock-controlled output rhythms.

Next, we monitored the effect of *EIP1* mutation on the expression pattern of three core oscillator genes, *CCA1*, *LHY*, and *TOC1*. In both LL and continuous dark (DD) free-running conditions, *eip1-1* lengthens the period in transcription of the three

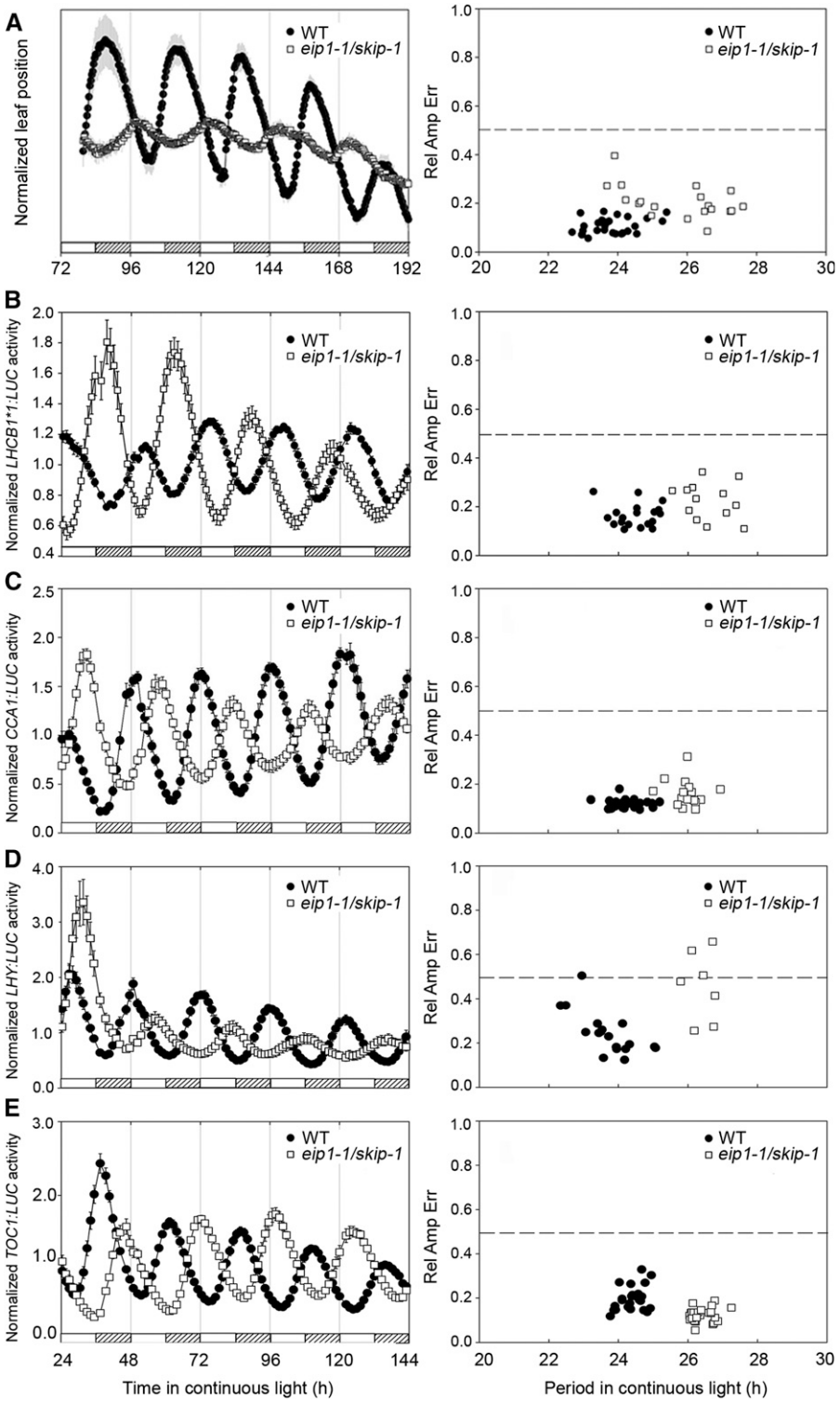


**Figure 1.** Effects of *SKIP* (*EIP1*) Mutation on Circadian Clock Outputs.

Mean traces (±SE) of cotyledon movement **(A)** or of luciferase activity from seedlings transformed with *LHCB1*1*:*LUC* **(B)**, *CCA1*:*LUC* **(C)**, *LHY*:*LUC* **(D)**, and *TOC1*:*LUC* **(E)** and scatterplots of RAE versus period length in *eip1-1/skip-1* ($n$ = 20) and the wild type (WT; $n$ = 30). Seedlings were entrained at 22°C in 12-h-light/12-h-dark photocycles for 7 d before release to LL (150 μmol $m^{-2}$ $s^{-1}$) at ZT = 0. RAE is a measure of the strength of the oscillation, with RAE = 0 corresponding to a perfect sine wave and RAE = 1 defining the lower limit of statistically significant rhythmicity. One-way analysis of variance was used for statistical analysis of period length, and in each case the period of *eip1-1/skip-1* was longer than that of the wild type ($P < 0.001$). Hatched bars represent subjective night, and blank bars represent subjective day.

oscillator genes, as measured with *Promoter*:*LUCIFERASE* (*LUC*) assays (Figures 1C to 1E; see Supplemental Figure 1 and Supplemental Table 2 online). The elongated period of *CCA1*, *LHY*, and *TOC1* expression was further confirmed at the level of steady state mRNA abundance by RNA gel blot analysis and quantitative RT-PCR (qRT-PCR) (see Supplemental Figure 2 online). Thus, these results indicate that *EIP1* is critical for the function of the *Arabidopsis* circadian clock.

### *EIP1* Encodes a Conserved SNW Domain–Containing Protein, SKIP, and Its Expression Is Global and Constitutive

*EIP1* (At1g77180) was isolated through a map-based cloning approach (the T-DNA was not linked to the mutation) and a 22-bp deletion was detected in *eip1-1* (see Supplemental Figure 3A online). At1g77180 previously has been identified as *SKIP* on the basis of altered abiotic stress responses (Lim et al., 2010); therefore, we rename *EIP1* as *SKIP* and *eip1-1* as *skip-1*. The *skip-1* mutation did not abolish the expression of *SKIP* (see Supplemental Figure 4 online). The *SKIP* transcript in *skip-1* has a 22-nucleotide deletion that results in a frame shift and is predicted to result in a truncated protein that retains the whole SNW and nuclear localization sequence domains and may retain partial function (see Supplemental Figure 3D online). A T-DNA insertion allele, *skip-2*, in which the T-DNA inserted into the nuclear localization sequence domain and therefore is predicted to result in a null phenotype was viable as a heterozygote but was severely dwarfed and infertile when homozygous (see Supplemental Figure 3D online). These results suggest that *SKIP* is an essential gene and that *skip-1* is a weak allele, but *skip-2* is a strong and presumably null allele. Because *skip-1* is inherited recessively, we do not favor the alternate hypothesis that *skip-1* is a neomorphic allele. *SKIP* encodes a 613–amino acid SNW/SKIP domain protein that is phylogenetically conserved from fungi to humans (see Supplemental Figures 3B and 3C online) and is an ortholog of SKIP in humans, Prp45 in yeast, and Bx42 in *Drosophila* (Saumweber et al., 1990; Albers et al., 2003; Zhang et al., 2003; Brès et al., 2005; Scott and Plon, 2005; Gahura et al., 2009).

The circadian clock defects in *skip-1* were completely complemented by transforming *SKIP* genomic DNA into *skip-1* plants (see Supplemental Figure 5A online), which confirms that *SKIP* is responsible for the circadian clock defects in *skip-1*. We performed green fluorescent protein (GFP)-tagged SKIP reporter, *SKIP* promoter-driven β-glucuronidase (GUS), and qRT-PCR assays to explore the subcellular localization and the expression pattern of *SKIP*. The results show that *SKIP* is a nuclear-localized protein with a broad expression pattern (Figures 2A to 2C).

Not all genes associated with the circadian clock exhibit circadian control of expression. We did not observe cycling abundance of *SKIP* steady state mRNA by RNA gel blot and qRT-PCR analysis (Figures 2D and 2E).

### SKIP Promotes Light Input and Affects the Sensitivity of the Clock to Light Resetting

Light and temperature are the most extensively studied input signals of the clock system. Light/dark cycles mediate circadian entrainment through associated photoreceptors, which regulate the abundance and/or activity of clock components. Therefore, we examined the function of SKIP in light input to the clock. The period of circadian rhythms in plants and day-active animals is inversely proportional to the environmental light intensity, known as Aschoff's rule (Aschoff, 1979). We observed that *skip-1* is hypersensitive to both red and blue light compared with the wild type because the mutant exhibited a steeper slope in a plot of period versus fluence rate (Figure 3A; see Supplemental Table 3 online); analysis of covariance showed slopes for *skip-1* to be significantly steeper than those of the wild type for both red ($P < 0.0015$) and blue ($P < 0.0001$) light. Like many clock mutants, *skip-1* also showed defects in photomorphogenesis, with a shorter hypocotyl in constant red (cRL) or constant blue (cBL) light conditions (Figure 3B). These phenotypes were completely rescued in *skip-1* complementation lines (see Supplemental Figure 5B online). Therefore, *SKIP* negatively regulates the inhibition of hypocotyl elongation in response to both red and blue light. These data reveal that *SKIP* plays a role in red and blue light input to the clock and in photomorphogenesis.

The circadian clock is able to modulate its own sensitivity to environmental stimuli, such as dawn or dusk and temperature changes. Thus, the ability of a given stimulus (e.g., light pulse) to shift the phase of the clock varies according to the time of day (Johnson, 1999). To confirm the function of SKIP in light signal transduction to the clock, we developed phase transition curves (PTCs) and phase response curves (PRCs) to pulses of red (30 min at 100 μmol $m^{-2}$ $s^{-1}$) or blue (30 min at 25 μmol $m^{-2}$ $s^{-1}$) light given to dark-adapted *skip-1* and wild-type plants by monitoring the expression of *CCA1*. We represented the PRC data as PTCs, in which the new phase, converted to circadian time (CT; which represents phase normalized to an arbitrary 24-h day), was plotted against the CT of the light pulse (Nagoshi et al., 2004; Locke et al., 2005). The PTCs showed that *skip-1* was more sensitive to light pulses in the late night/early morning than the wild type (Figure 3C; see Supplemental Table 4 online), indicating that *skip-1* is hypersensitive to both red and blue light and SKIP negatively regulates clock sensitivity to light resetting. As can be seen in the PRCs, *skip-1* exhibited stronger (by ~3 h) phase advances to pulses given in the subjective day and stronger (by ~3.5 h) phase delays to red light pulses given in the subjective night (see Supplemental Figure 6 and Supplemental Table 4 online). For blue light pulses, *skip-1* exhibited stronger (by ~2.4 h) phase advances to pulses given in the subjective day and dramatically greater phase delays to pulses given in the subjective night (see Supplemental Figure 6 and Supplemental Table 4 online).

### SKIP Is Required for Maintaining Temperature Compensation

Organisms are able to maintain a circadian period close to 24 h across a broad range of physiological temperatures, which is known as temperature compensation and is one of hallmarks of circadian clocks (Zimmerman et al., 1968). The lengthened period phenotype of *skip-1* was temperature sensitive and gradually disappeared with increasing temperature from 17 to 27°C (Figure 4). The period length in *skip-1* was ~3.5 h longer than that of the wild type at 17°C but very close to the wild type at 27°C (Figure 4). Thus, *skip-1* has partially lost temperature compensation,

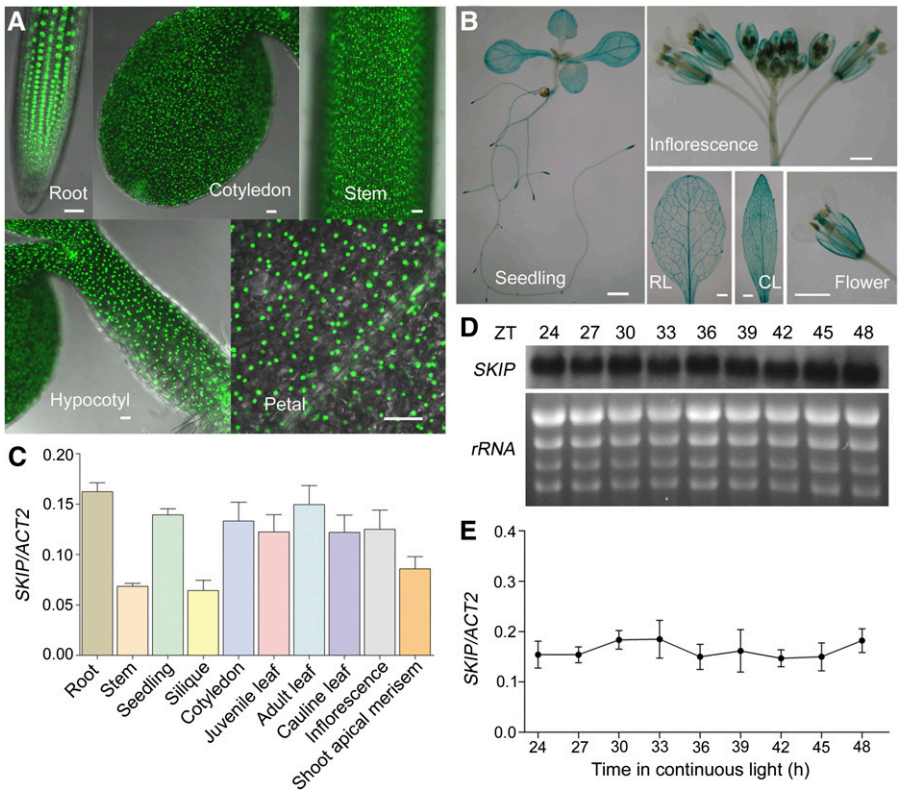


**Figure 2.** Expression, Subcellular Localization, and Circadian Regulation of *SKIP*.

**(A)** Expression of *SKIP* as determined by confocal microscopy of *SKIP*:*GFP-SKIP*/*skip-1* transgenic lines. Samples were collected at ZT6 (6 h after dawn). Bars = 40 μm.

**(B)** *SKIP* expression in plants expressing *SKIP*:*GUS*. CL, cauline leaf; RL, rosette leaf. Bars = 1 mm.

**(C)** Expression of *SKIP* in seedlings and different organs by qRT-PCR assay. Samples were collected at ZT6. The values are the mean ± SD from three biological independent experiments.

**(D)** Expression of *SKIP* under free-running conditions detected by RNA gel blots. Seedlings were entrained at 22°C in 12-h-light/12-h-dark photocycles for 7 d before release to LL (150 μmol $m^{-2}$ $s^{-1}$) at ZT = 0. Samples were harvested after 24 h in LL and every 3 h thereafter for the next 24 h. Total RNA was assayed by RNA gel blot hybridization with *SKIP*-specific probes. Two biological replicates were performed with similar results, and the result from one of the experiments is shown.

**(E)** Expression of *SKIP* under free-running conditions measured by qRT-PCR. Abundance of *SKIP* total mRNA was measured from seedlings entrained at 22°C in 12-h-light/12-h-dark photocycles for 7 d before release to LL (150 μmol $m^{-2}$ $s^{-1}$) and harvested at ZT = 24 through qRT-PCR. The values are the mean and SD from three biological replicates. There was no significant difference over time among the expression level of *SKIP* as determined by Tukey's multiple comparison test ($P < 0.05$).

indicating that SKIP plays a critical role in maintaining temperature compensation of the circadian clock.

### SKIP Is a Splicing Factor and One of the Components of the Spliceosome in Planta

It is well documented that SKIP acts as a splicing factor in both mammals and yeast (Albers et al., 2003; Bessonov et al., 2008; Chen et al., 2011). To investigate further the molecular mechanism by which SKIP affects circadian clock function in *Arabidopsis*, we asked whether SKIP functions as a splicing factor.

We first tested the ability of *SKIP* to complement the yeast *prp45(1-169)* mutant, which is defective in cell division and exhibits temperature sensitivity of growth due to a defect in pre-mRNA splicing (Gahura et al., 2009). *ADH1*:*SKIP* was able to rescue the cell division and temperature-dependent growth arrest defects in *prp45(1-169)* (Figures 5A and 5B).

To examine further whether SKIP acts as a splicing factor like Prp45 in yeast, we introduced the plasmids expressing an unmutated *ACT1-CUP1* fusion construct or an *ACT1-CUP1* fusion construct containing mutations in the 5′ splice site (5′SS), branch point site (BPS), or the 3′ splice site (3′SS) region of the *ACT1* intron as indicated (Figure 5C) into *prp45(1-169)*. Levels of pre-mRNA, lariat-exon 2 intermediate, and mature mRNA are analyzed by primer extension. Consistent with a previous report (Gahura et al., 2009), the splicing efficiency of unmutated *ACT1-CUP1* fusion template in the *prp45(1-169)* appears the same as in the wild type *(PRP45)* (Figure 5D, lanes 1 and 2), and the splicing efficiency is not altered by transforming *prp45 (1-169)* with *SKIP* (Figure 5D, lanes 1 to 3). However, the splicing

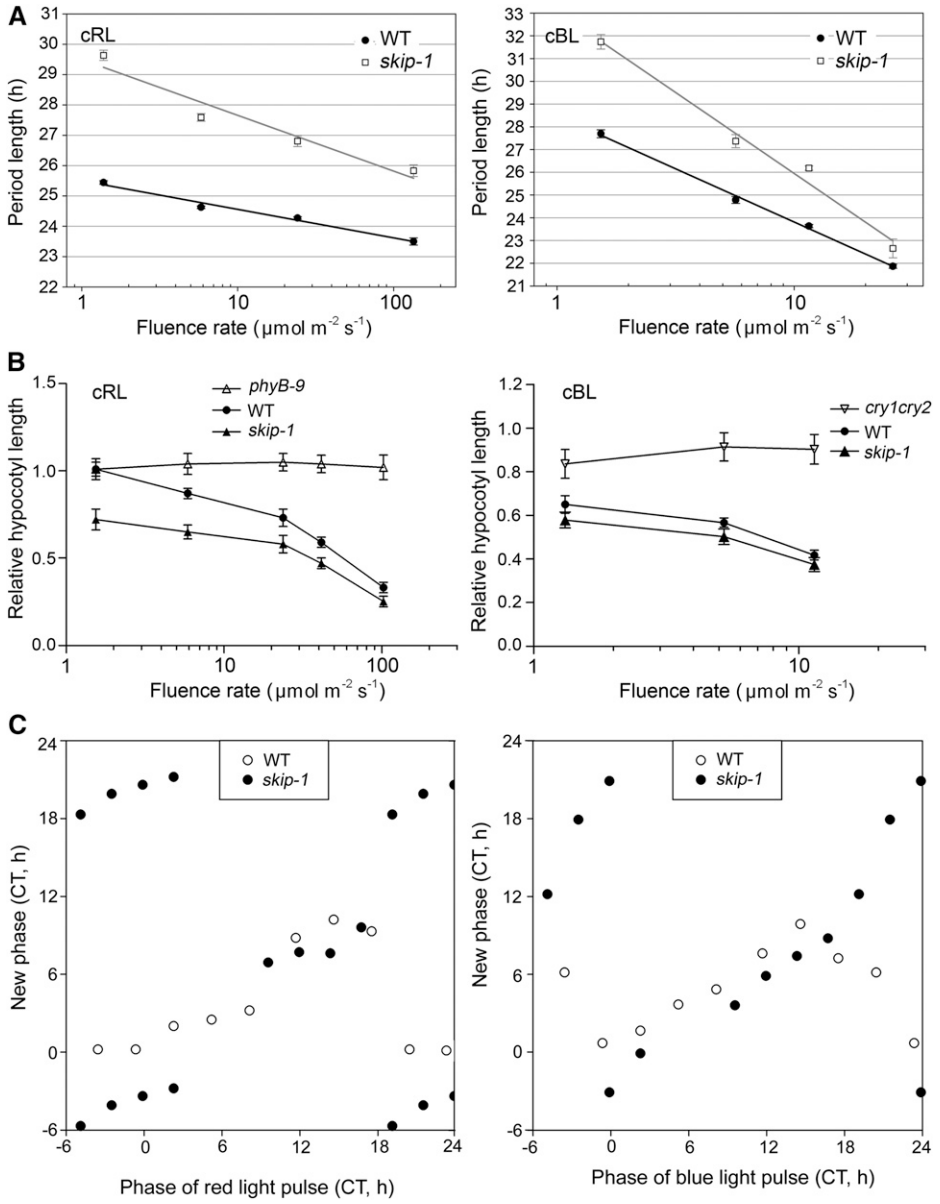


**Figure 3.** SKIP Mediates Light Input to and Resetting the Circadian Clock.

**(A)** Fluence response curves of *CCA1:LUC* period in *skip-1* and wild-type (WT) plants under cRL or cBL conditions.

**(B)** Hypocotyl elongation is hypersensitive to light inhibition in cRL or cBL light in *skip-1* relative to the wild type. The values are mean ± SE from three independent experiments.

**(C)** PTCs. Data from Supplemental Figure 6 and Supplemental Table 4 online are replotted as PTCs in which the new acrophase (peak phase) of *CCA1:LUC* expression is plotted against the time of pulses of red or blue light. The slope of the curve is closer to 1 than to 0; hence, this represents type 1 (weak) resetting.

efficiency for the mutated templates, including 3′SS UAG to gAG, 5′SS GUA to GUc, and BPS (UACUAAC to UACUAcC or UACUAgC), was compromised in *prp45(1-169)* but was partially rescued by introducing the *SKIP* gene into *prp45(1-169)* (Figure 5D, lanes 4 to 15). That SKIP is able to rescue the cell division, temperature-sensitive, and splicing efficiency defects of *prp45 (1-169)* in yeast indicates that SKIP is functionally conserved and possesses splicing activity in yeast.

Pre-mRNA is spliced to generate mature mRNA within a ribonucleoprotein complex termed the spliceosome. To address whether SKIP is a component of the spliceosome in planta, we employed fluorescence resonance energy transfer (FRET) to test for colocalization and physical interaction of SKIP with the spliceosome components U1-70K (Golovkin and Reddy, 1996) and SR45 (Ali et al., 2007) in *Nicotiana benthamiana*. SKIP co-localized in nuclear speckles with the spliceosome components

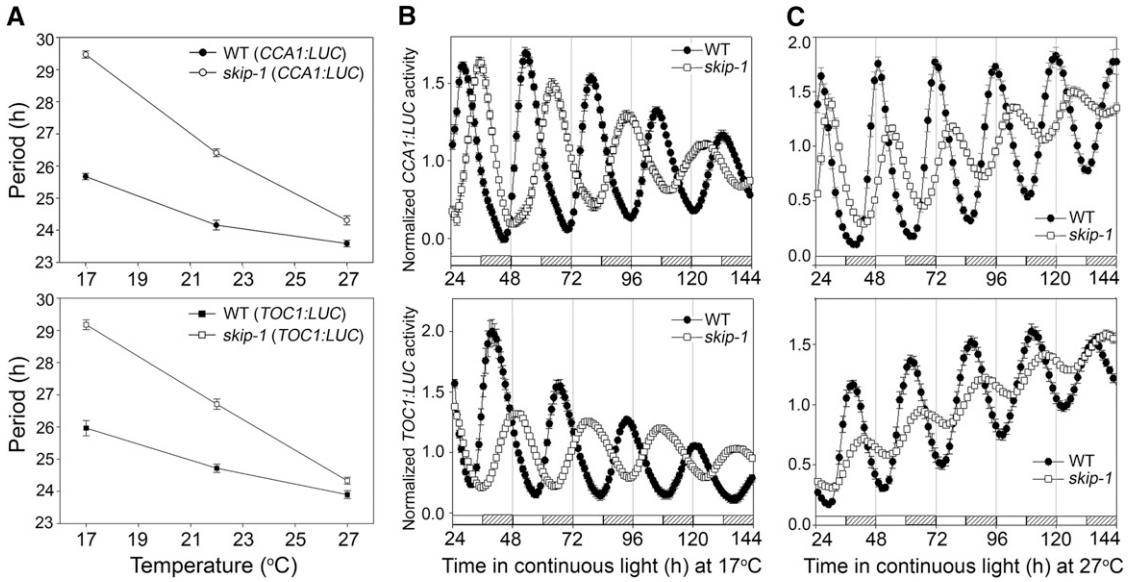


**Figure 4.** SKIP Is Involved in Maintaining Temperature Compensation of the Clock.

**(A)** Period length of *CCA1*:*LUC* (top panel) and *TOC1*:*LUC* (bottom panel) at 17, 22, and 27°C for the wild type (WT; closed symbols) and *skip-1* (open symbols). The values are the mean ± SD from three biological independent experiments.
**(B)** Luciferase activity (mean ± SE) of two independent transgenic lines for the wild type (closed symbols) and *skip-1* (open symbols) carrying *CCA1*:*LUC* (top panel) or *TOC1*:*LUC* (bottom panel) at 17°C in continuous light. White and gray bars at bottom indicated subjective day and night, respectively.
**(C)** Luciferase activity (mean ± SE) of two independent transgenic lines for the wild type (closed symbols) and *skip-1* (open symbols) carrying *CCA1*:*LUC* (top panel) or *TOC1*:*LUC* (bottom panel) at 27°C in continuous light. White and gray bars at bottom indicated subjective day and night, respectively.

U1-70K and SR45 (Figures 6A and 6B). No FRET signal was detected in cells cotransformed with GFP-SKIP and U1-70K-mCherry (Figure 6A), indicating that these proteins do not interact closely. However, a strong FRET emission was observed in nuclear speckles of cells coexpressing GFP-SKIP and SR45-mCherry proteins (Figure 6B). The results were further confirmed by photobleaching. In agreement with the above results, FRET between GFP-SKIP and SR45-mCherry was detectable before bleaching the SR45-mCherry energy acceptor (Figure 6C, the prebleach panel), but enhanced fluorescent intensity of GFP-SKIP was observed after photodestruction of SR45-mCherry (Figure 6C, the postbleach panel), indicating energy transfer between GFP-SKIP and SR45-mCherry (Figure 6C). Increased GFP:SKIP fluorescence intensity after photobleaching of the mCherry acceptor is quantified in Figure 6D. These results indicate that SKIP is a component of the spliceosome in which it is closely associated with SR45.

### Mutation of *SKIP* Causes Genome-Wide Splicing Defects in *Arabidopsis*

To investigate further the function of SKIP in mRNA metabolism, we performed ultra-high-throughput RNA sequencing (RNA-seq) analysis using a mutant carrying the strong *skip-2* loss-of-function allele. About 14.47 and 15.76 million reads with an average length of 42 bp from the wild type and *skip-2*, respectively, were aligned to the *Arabidopsis* reference genome (TAIR 9) (see Supplemental Table 5 online). Among them, ~11.95 and 14.76 million reads for the wild type and *skip-2*, respectively, were mapped to unique loci in the genome (see Supplemental Table 5 online). An additional 0.34 and 0.48 million reads for the wild type and *skip-2*, respectively, were aligned to annotated exon-intron junctions (see Supplemental Table 5 online). Compared with the wild type, in *skip-2*, we identified ~2979 novel splicing events, which could be sorted into four categories: intron retention (IR), alternative 5′ or 3′ splice site (A5′SS or A3′SS), and exon skipping (ES) (Figure 7A; see Supplemental Data Set 1 online). Although examples of both IR and ES were detected, the majority of the altered splicing events involved the use of alternative donor and acceptor splice sites, indicating that SKIP is probably involved in splice site recognition.

We validated these observations by detecting representative IR, A5′SS, A3′SS, and ES novel splicing events in *skip-2* through RT-PCR using primers flanking them (see Supplemental Table 6 online). The IR, A5′SS, A3′SS, and ES events sampled from each chromosome could be detected in *skip-1* and *skip-2*, but not in the wild type (Figures 7B to 7F; see Supplemental Figure 7 online).

Consensus sequences at the 5′SS and 3′SS are important for accurate splicing of pre-mRNAs in plants (Reddy, 2007). Although the majority of splice sites used in *skip-2* conformed to consensus, the frequency distribution of the nucleotides at 5′SS and 3′SS from the novel splicing events detected in *skip-2* differed from consensus, with obvious decreases in the frequency of both the dominant G and T at +1 and +2 positions of 5′ alternative donor sites and of both the A and G at −2 and −1 positions of 3′ alternative acceptor sites, consistent with a role of SKIP protein in 5′SS and 3′SS recognition or cleavage (Figure 7G; see Supplemental Data Set 2 online).

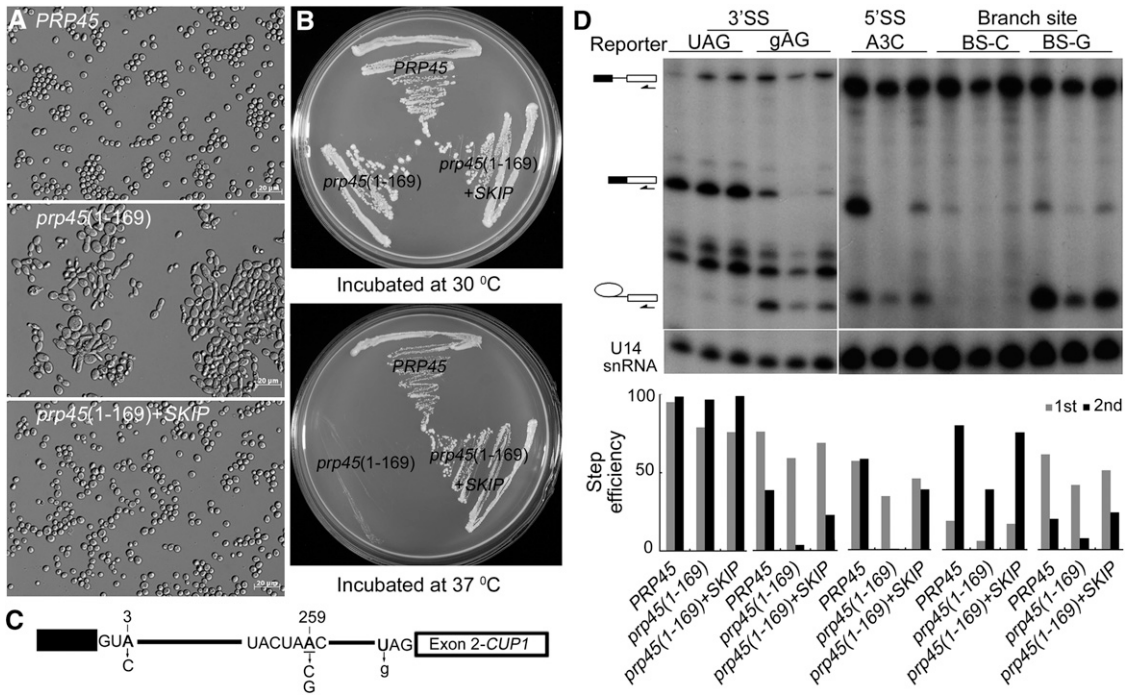


**Figure 5.** At-*SKIP* Is Able to Complement Morphologic, Temperature-Sensitive, and Splicing Efficiency Defects of *prp45*(1-169) in Yeast.

**(A)** Cell morphologies of *PRP45*, *prp45*(1-169), and *prp45*(1-169)+*SKIP*.

**(B)** The growth of cells from *PRP45*, *prp45*(1-169), and *prp45*(1-169)+*SKIP* at 30 and 37°C.

**(C)** Schematic of *ACT1-CUP1* pre-mRNA and its mutation sites as used in **(D)**. Mutations of the *ACT1-CUP1* pre-mRNA in the 5′SS, BPS, or the 3′SS region of the *ACT1* intron are shown. gAG is the mutated 3′SS of UAG. A3C represents the 5′SS GUA- to-GUC mutation. BS-C and BS-G is the 259-bp mutation of branch site from A to C and G, respectively.

**(D)** *SKIP* rescues the *prp45*(1-169) splicing deficiency phenotype as observed through primer extension analysis. The abundances of pre-mRNA (P; top), mRNA (M; middle), and lariat intermediate (LI; bottom) were estimated with Quantity One. The first-step efficiency (gray bars) and the second step efficiency (black bars) were calculated with (M+LI)/(P+M+LI) and M/(M+LI), respectively. Three biologically independent experiments were conducted, similar results were obtained, and the results from one replicate are shown.

To identify biological pathways in which SKIP is involved, we conducted Gene Ontology analysis of genes undergoing abnormal splicing in *skip-2* mutants through the agriGO Web server (Du et al., 2010). The results show that SKIP may be involved in multiple biological processes, including many aspects of metabolism, development, and reproduction (see Supplemental Figure 8A online). All the categories observed were overrepresented relative to the percentage in the genome (see Supplemental Figure 8B online).

### SKIP Is Involved in the Pre-mRNA Splicing of Oscillator Genes in *Arabidopsis*

To determine whether SKIP directly regulates the expression of clock genes through splicing, we measured alternative splicing of *PRR7* and *PRR9* by an electrophoretic approach. In *skip-1*, aberrantly spliced variants of *PRR7* and *PRR9* were increased compared with the wild type (see Supplemental Figures 9A and 9B online).

To determine whether patterns of alternative splicing of *PRR7* and *PRR9* mRNAs are regulated by the circadian clock, we further performed qRT-PCR to detect the expression of the multiple *PRR7* and *PRR9* splicing isoforms. The *skip-1* mutation decreased the accumulation of the fully spliced *PRR7_a* isoform and increased the accumulation of *PRR7_b* and *PRR7_c* aberrantly spliced variants (Figures 8A to 8C). Similarly, the accumulation of the fully spliced *PRR9_a* isoform was decreased, whereas the accumulation of *PRR9_b*, *PRR9_c*, *PRR9_d*, and *PRR9_e* incompletely spliced isoforms was elevated in *skip-1* compared with the wild type (Figures 8D to 8H). These splicing defects in *skip-1* resulted in an ~50% reduction in the peak level of *PRR7_a* and a slight reduction in the peak level of *PRR9_a*, the only isoforms capable of being translated to give functional PRR7 and PRR9 proteins (Figures 8A and 8D). The splicing defects also reduced the proportion of *PRR7_a* and *PRR9_a* relative to total *PRR7* and *PRR9* transcripts in *skip-1* (Figures 8A to 8H; see Supplemental Figures 9C and 9D online). These results suggest that the decreased peak levels of *PRR7_a* and, to a lesser extent, *PRR9_a* and possibly the enhanced accumulation of the aberrantly spliced *PRR7* and *PRR9* isoforms in *skip-1* contribute to the lengthened period phenotype, which is consistent with the lengthened period seen in *prr7* and *prr9* loss-of-function mutants (Michael et al., 2003; Farré et al., 2005; Salomé and McClung, 2005).

Splicing of pre-mRNA requires recruitment to the spliceosome. Therefore, we asked if pre-mRNAs associate with SKIP in planta using the circadian oscillator genes *PRR7* and *PRR9* as examples. We took advantage of the *SKIP*:*GFP-SKIP* transgenic

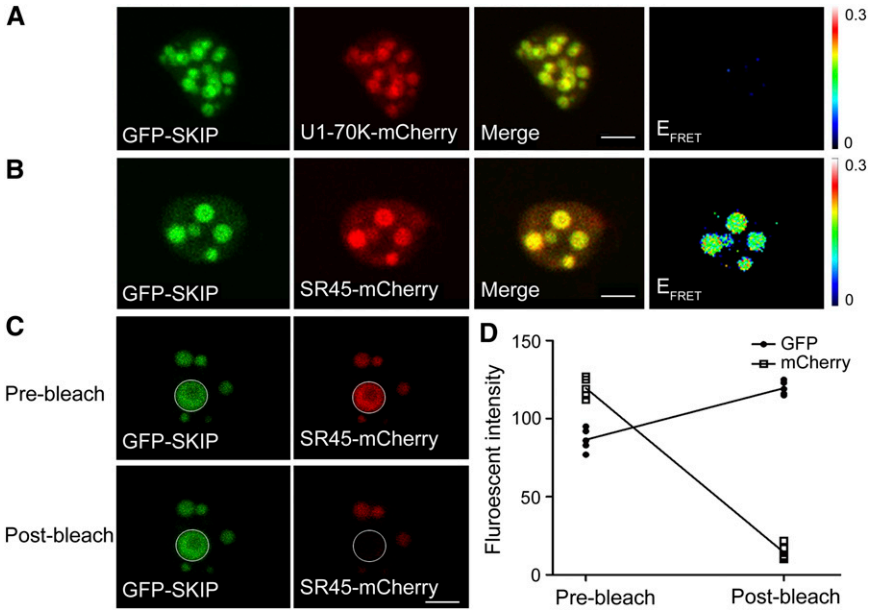


**Figure 6.** SKIP Is a Component of the Spliceosome and Interacts with SR45.

**(A)** Colocalization of SKIP with U1-70K in vivo by sensitized emission assay. Bar = 5 μm.
**(B)** Colocalization and interaction of SKIP with SR45 in vivo by sensitized emission assay. Bar = 5 μm.
**(C)** Colocalization and interaction of SKIP with SR45 in vivo by photobleaching assay. Images from GFP, mCherry, and FRET channels before and after SR45-mCherry photobleaching using illumination at 543 nm. Bar = 5 μm.
**(D)** Emission of donor and acceptor images with acceptor photobleaching FRET. The fluorescent intensity of pre- and postbleach images from donor and acceptor was calculated with Image J, and it was normalized to the nonbleached region. Five independent photobleaching results are shown.

line in the *skip-1* background and applied antibody against GFP to immunoprecipitate GFP-SKIP. The immunoprecipitates of GFP-SKIP were then reverse transcribed into cDNA and further probed by RT-PCR with primers specific to *PRR7* and *PRR9*, using no immunoprecipitation (input) and immunoprecipitation without anti-GFP antibody (NA) samples as controls. Pre-mRNA for each of these clock genes was detected in the input and the immunoprecipitation sample from the SKIP:GFP-SKIP transgenic line and confirmed by sequencing (Figure 8I). The results support a role for the SKIP-containing spliceosome in splicing of the *PRR7* and *PRR9* pre-mRNAs.

To determine whether SKIP modulates circadian period solely through alternative splicing of *PRR7* and *PRR9*, we generated double or triple mutants of *prr7-3*, *prr9-1*, and *skip-1* and assessed circadian rhythmicity with *CCA1:LUC*. The periods of *prr7-3 skip-1* and *prr9-1 skip-1* double mutants were significantly longer than those of *prr7-3*, *prr9-1*, and *skip-1* single mutants but were significantly shorter than that of the *prr7-3 prr9-1* double mutant, which suggests that the *skip-1* mutation partially compromises the expression of both *PRR7* and *PRR9*, but the defect is not as severe as a complete loss of *PRR7* and *PRR9* function. This is consistent with the reduced but still detectable levels of *PRR7_a* and *PRR9_a* mRNAs (Figure 8J). Moreover, there must be circadian clock targets in addition to *PRR7* and *PRR9* because the period of the *prr7-3 prr9-1 skip-1* triple mutant was significantly longer than that of the *prr7-3 prr9-1* double mutant (Figure 8J). Consistent with this prediction, we observed *skip-1* splicing defects for several other clock genes, including *ARR4*, *CCA1*, *LHY*, and *TOC1*, although not obvious for *FIO1*, *TEJ*, and *ARR3* under the same condition (see Supplemental Figures 9E and 9F online). We conclude that the splicing defects in other clock genes besides *PRR7* and *PRR9* may also contribute to the elongated period or other circadian defects of *skip-1*. It was observed that the splicing patterns for *LHY*, *PRR9*, *TEJ*, and *FIO1* in the wild type are quite dissimilar from those in *skip-2* determined with RNA-seq (see Supplemental Figure 9E online). We attribute this to low expression in the wild type; the period difference between the wild type and *skip-2* resulted in sampling at the peak of expression in *skip-2* but at the trough of expression in the wild type.

We initially identified *skip-1* on the basis of a flowering time defect, so we also assessed splicing of the transcripts of flowering time genes, including *SUPPRESSOR OF OVEREXPRESSION OF CO1* (*SOC1*), *CONSTANS*, *FLOWERING LOCUS T* (*FT*), *ELF3*, *ELF4*, and *GI*. Among these genes, we observed obvious splicing defects (IR) for *ELF3* and *GI* in *skip-1* compared with the wild type (see Supplemental Figures 9E and 9F online), suggesting that SKIP may affect both circadian clock and flowering time through alternative splicing. Loss of ELF3 function through IR would be consistent with the early flowering phenotype (Zagotta et al., 1996) characteristic of *skip* mutants, although loss of GI function would be expected to confer late flowering (Rédei, 1962; Koornneef et al., 1991). However, the abundance of the mature fully spliced transcript was not obviously reduced in *skip-1* for either *ELF3* or *GI*, suggesting that

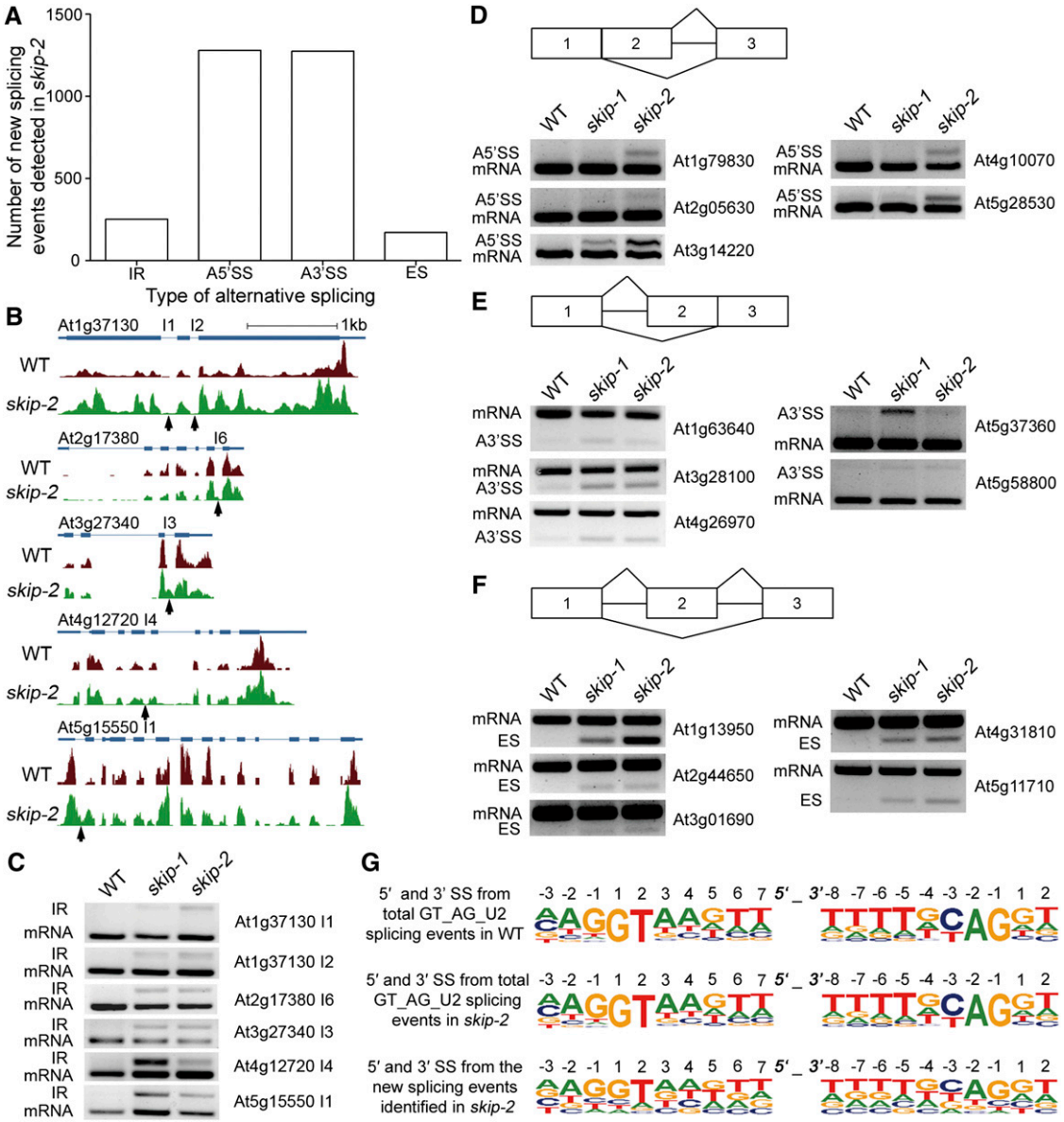


**Figure 7.** Genome-Wide Effects of *SKIP* Mutation on Alternative Splicing.

**(A)** Frequency of new splicing events detected by RNA-seq in *skip-2*.
**(B)** Pre-mRNAs with IR splicing defects in *skip-2* detected by RNA-seq. One gene from each chromosome was randomly picked as representative. Arrows indicate retained intron in *skip-2*. WT, the wild type.
**(C)** to **(F)** Validation of the selected genes with IR **(C)**, A5′SS **(D)**, A3′SS **(E)**, or ES **(F)** splicing defects by RT-PCR in the wild type, *skip-1* and *skip-2*.
**(G)** The frequency distribution of nucleotides at consensus 5′ and 3′SSs. Sequence logos illustrate consensus sequences for splice sites in the wild type (top logos), *skip-2* (middle logos), and for novel splice sites detected in *skip-2* (bottom logos).

these transcripts are unlikely to be the primary SKIP targets of relevance for the early flowering phenotype seen in *skip-1* mutants.

## DISCUSSION

To date, most studies of the circadian clock network in plants have emphasized transcriptional and posttranslational regulatory mechanisms. Recent genome-wide gene expression analyses have suggested that mRNA splicing is under the control of the circadian clock (Hazen et al., 2009), and it has been demonstrated that pre-mRNAs of several clock genes, including *CCA1*, *LHY*, *PRR7*, and *PRR9*, undergo alternative splicing (Filichkin et al., 2010; Sanchez et al., 2010; James et al., 2012). PRMT5 has been shown to be important for correct alternative splicing of *PRR9* (Hong et al., 2010; Sanchez et al., 2010), but splicing components necessary for correct alternative splicing of these

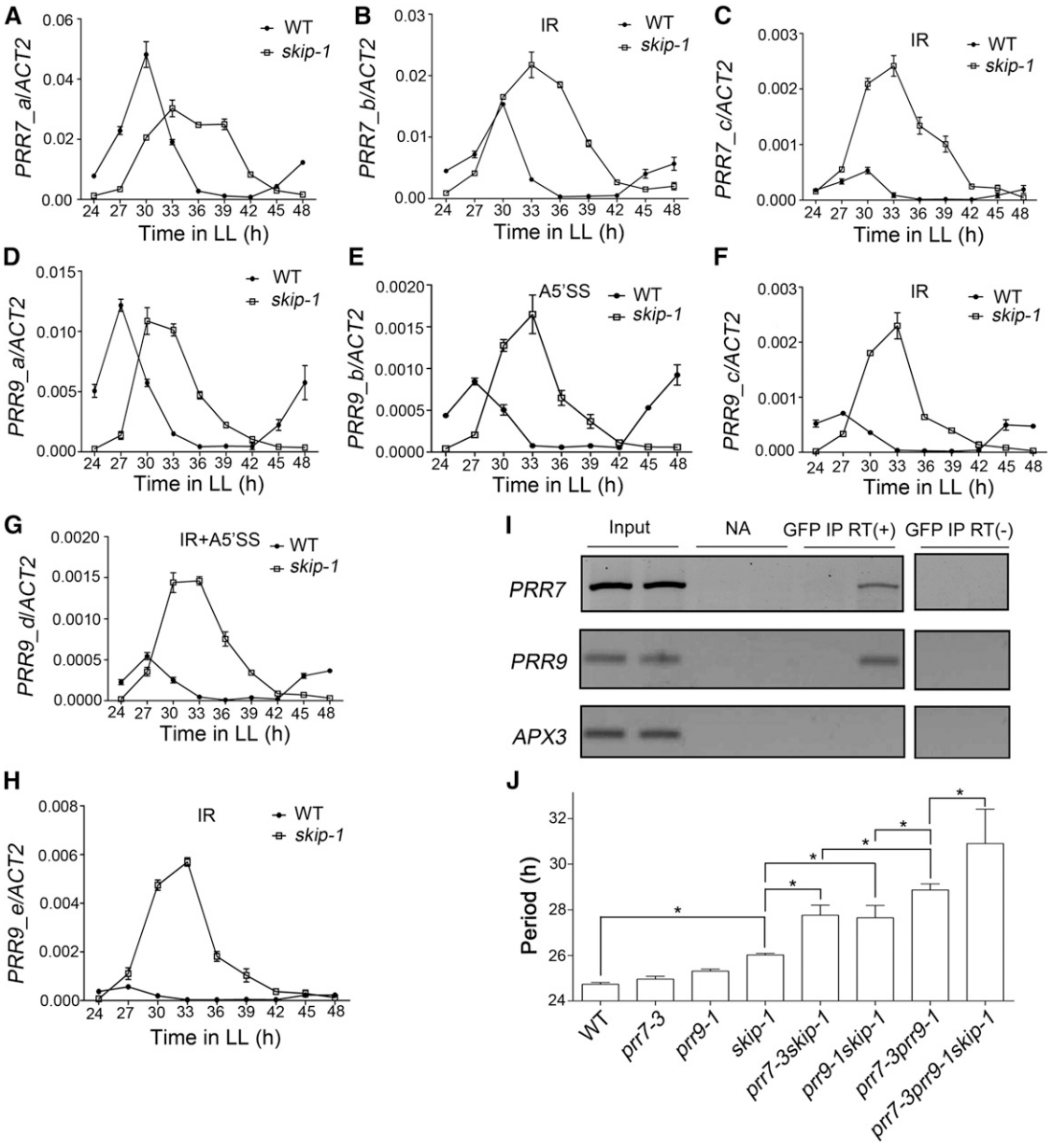


**Figure 8.** SKIP Is Required for Regulating the Alternative Splicing and Function of *PRR7* and *PRR9*.

Splicing variants of *PRR7* (**[A]** to **[C]**) and *PRR9* (**[D]** to **[H]**) as detected by qRT-PCR. Seedlings in continuous light were entrained in 12-h-light/12-h-dark photocycles for 7 d and transferred to LL prior to harvest at the indicated times. The values are the mean and SD from three biological independent experiments. WT, the wild type.

**(I)** RNA-IP analysis reveals that SKIP binds to the pre-mRNAs of *PRR7* and *PRR9* but not to the pre-mRNA of *APX3*. Detection of SKIP-associated pre-mRNA by RT-PCR. For Input, NA (no antibody), GFP-IP RT (+), and GFP-IP RT (−), the left lane is the wild type and the right lane is a complemented *SKIP*:*GFP-SKIP*/*skip-1* T3 transgenic line. GFP-IP RT (+) or (−) is the PCR performed with the templates directly eluted from RNA-IP against GFP with reverse transcription [RT(+)] or without reverse transcription [RT(−)].

**(J)** Genetic analysis of circadian period length in the wild type and in single, double, and triple mutants of *prrr7-3*, *prr9-1*, and *skip-1* through detecting the LUC activity of *CCA1*:*LUC* (*Tukey's multiple comparison test, $P < 0.05$).

and other clock genes remain only incompletely known. Our study identifies SKIP as a splicing factor important for full splicing of *PRR7* and *PRR9* and other clock gene pre-mRNAs.

### SKIP, a Splicing Factor, Is Required for Normal Function of the Clock

We identified SKIP, a single-copy gene in *Arabidopsis*, through a forward genetic analysis on the basis of a partial loss-of-function early-flowering and photoperiod-insensitive phenotype. Because other mutations with similar phenotypes often affect circadian clock function, we assessed circadian rhythms in wild-type and *skip-1* plants and found that defects in *SKIP* lengthen circadian period of both clock-controlled output rhythms as well as of transcription of the core oscillator genes *CCA1*, *LHY*, and *TOC1* (Figure 1). Thus, *SKIP* is critical for circadian period determination in *Arabidopsis*. Furthermore, the *skip-1* long period phenotype exhibits temperature sensitivity, indicating that *SKIP* is required for temperature compensation of circadian period length (Figure 4). In addition, *SKIP* also modulates clock entrainment to light input and negatively regulates the inhibition of hypocotyl elongation in response to red and blue light (Figure 3). Taken together, our results suggest that *SKIP* is important for clock function in the *Arabidopsis*.

### SKIP Acts as a Spliceosomal Component Important for Alternative Splicing

SKIP is evolutionarily conserved, with close homologs in yeast and mammals. SKIP plays important roles as a transcriptional coactivator/corepressor in mammals (Scott and Plon, 2005; Brès et al., 2009). However, a recent proteomic analysis of the spliceosome identified SKIP as part of the Prp19-related complex or Nineteen Complex in yeast (Bessonov et al., 2008). Consistent with this observation, human SKIP acts as a splicing factor to specifically regulate alternative splicing and expression of *p21* (Chen et al., 2011). SKIP interacts with the 3′SS recognition factor U2AF65 and recruits it to the *p21* mRNA in vivo, and down-regulation of SKIP induces a rapid repression of *p21* expression via reduced splicing of the first or second *p21* introns, resulting in subsequent *p53*-mediated apoptosis (Chen et al., 2011).

The yeast SKIP homolog, Prp45, is a component of the spliceosomal Nineteen Complex and functions as a splicing factor (Gahura et al., 2009). Weak *prp45* alleles cause defects in the splicing of actin and other genes, resulting in temperature-sensitive growth, while strong *prp45* alleles are lethal (Figueroa and Hayman, 2004; Gahura et al., 2009).

In plants, the molecular mechanisms by which SKIP functions are incompletely established. We have shown that SKIP rescues both alternative splicing and temperature-sensitive growth defects in *prp45*-mutated yeast (Figure 5), indicating that SKIP possesses similar properties to Prp45 as a splicing factor. Consistent with this, in planta SKIP colocalizes with the spliceosomal protein U1-70K and interacts physically with SR45 (Figure 6), a second component of the plant spliceosome (Ali et al., 2007; Tanabe et al., 2009). Therefore, we conclude that SKIP is a component of the *Arabidopsis* spliceosome.

Consistent with this role, we observe genome-wide defects in pre-mRNA splicing in *skip* mutants (Figure 7). Our analysis implicates *SKIP* in multiple biological processes, including post-embryonic development, protein metabolism, response to stress, reproductive development, and response to abiotic stimuli, which is consistent with an important role for SKIP in pre-mRNA splicing and for roles for alternative splicing in multiple biological processes (see Supplemental Figure 8 online). Others have established that SKIP is involved in abscisic acid signaling, as well as in salt and osmotic tolerance in *Arabidopsis* and rice (*Oryza sativa*), although these studies attributed the effects of SKIP misexpression primarily to roles in transcriptional regulation (Hou et al., 2009; Lim et al., 2010). Thus, we cannot rule out the possibility that SKIP regulates circadian clock function at the transcriptional level as well.

Consistent with its role in pre-mRNA splicing, aberrant splicing events in *skip-2* include examples of IR and ES, and, most commonly, alternative 5′ donor and 3′ acceptor splice site selection (Figure 7; see Supplemental Figures 7 and 9 online). The nucleotide sequences of these novel 5′SS and 3′SSs diverge considerably from consensus, indicating that SKIP plays an important role in the utilization of splice donor and acceptor sites that diverge from consensus (Figure 7G), although this role could be associated with splice site recognition, cleavage, or both. Consistent with a role in cleavage, SKIP is a component of splicing complexes B and C, which catalyze both 5′SS and 3′SS cleavage (Bessonov et al., 2008), and SKIP interacts with the 3′SS recognition factor U2AF65 to regulate splicing and expression of p21 gene in mammals (Chen et al., 2011).

### SKIP Is Essential for Normal Function of the Circadian Clock through Modulating the Alternative Splicing of Clock Genes

The roles for splicing factors in circadian clock control are only incompletely elucidated. SKIP associates with the pre-mRNAs of *PRR7* and *PRR9* and is necessary for their clock-regulated splicing (Figure 8; see Supplemental Figure 9 online). Failure to fully splice *PRR7* and *PRR9* mRNAs may contribute to the long period seen in the *skip-1*, although there must be additional clock-relevant defects in the *skip-1* because a triple *prr7 prr9 skip-1* exhibits a longer period than does the *prr7 prr9* double mutant (Figure 8J; see Supplemental Figures 9E and 9F online). *PRR7*, *PRR9*, *LHY*, and *CCA1* all are important for proper temperature compensation of the *Arabidopsis* circadian clock (Salomé and McClung, 2005; Gould et al., 2006; Salomé et al., 2010), and alternative splicing of *LHY* and *PRR7* has been established as critical for proper temperature compensation (James et al., 2012). The temperature-sensitive period lengthening of *skip-1* may result from a temperature-sensitive splicing defect of one or more of these targets and suggests SKIP as a component of the temperature-sensitive alternative splicing mechanism.

In conclusion, our findings uncover a general role of a splicing factor, SKIP, for proper function of the circadian clock and provide a molecular link between the circadian clock and alternative splicing.

## METHODS

### Plant Materials and Growth Conditions

All plant materials used in this study were in the Columbia-0 ecotype (Col-0) background of *Arabidopsis thaliana*. Seeds were sterilized and placed on

Murashige and Skoog medium with 0.3% agar and 1% Suc. After stratification in the dark at 4°C for 2 d, plates were transferred to white light (70 μmol $m^{-2}$ $s^{-1}$) in a Percival CU36L5 growth chamber (Percival Scientific). Plants for flowering time determination were grown under various light–dark photocycles (LD) with cool white fluorescent light (100 μmol $m^{-2}$ $s^{-1}$) at 22°C for the day and 18°C for the night.

For hypocotyl length measurement, sterilized and stratified seeds were planted on Murashige and Skoog medium with 0.3% agar and 1% Suc plates under white light for 12 h before transfer into cRL (670 nm) or cBL (470 nm) at 22°C under various fluence rates, provided with a Percival E30LED chamber. Hypocotyl length was measured after 6 d in cRL and cBL.

### Leaf Movement and Bioluminescence Measurement

Leaf movement was measured as described previously (Kim et al., 2010). For LUC activity assays, 7- to 10-d-old seedlings entrained to LD (12 h light/12 h dark) were released into LL or DD conditions for LUC measurement (Plautz et al., 1997). Circadian rhythms were assayed with BRASS 2.1.4 (Southern and Millar, 2005), which employs fast Fourier transform nonlinear least squares (Plautz et al., 1997). The strength of a circadian rhythm is expressed as relative amplitude error (RAE). An ideal cosine wave is defined as RAE = 0 and RAE = 1 defines the statistically detectable limit of rhythmicity.

For temperature compensation assays, seedlings were entrained in 12-h-light/12-h-dark (LD) cycles at 22°C for 7 to 10 d before transferring to LL at 12, 22, and 27°C for LUC activity measurement.

For fluence response curves, *CCA1*:*LUC* transgenic seedlings were entrained to LD cycles at 22°C for 7 d before transfer to cRL or cBL at indicated fluence rates. On the first day in LL, seedlings were transferred to 96-well microplates (Perkin-Elmer) for LUC activity measurement; microplates were transferred manually to the Packard TopCount at 3-h intervals. The response of period to fluence rate of red and blue light was analyzed by linear regression followed by analysis of covariance using GraphPad Prism software.

PRCs were generated with *CCA1*:*LUC* seedlings entrained to 12-h-light/12-h-dark cycles at 22°C for 7 d before transferring to DD. After one whole day in DD, pulses (30 min) of red (100 μmol $m^{-2}$ $s^{-1}$) or blue (25 μmol $m^{-2}$ $s^{-1}$) light were given to individual plates at 3-h intervals scanning one complete circadian cycle (24 h). Free-running rhythms of *CCA1*:*LUC* were monitored in DD. Acrophase (peak phase) was determined by Fourier transform nonlinear least squares. Changes in acrophase relative to seedlings not exposed to light pulse are plotted against the CT of the light pulses. For CT, phase is normalized for period length to an arbitrary 24-h day, with CT0 defined as dawn (lights on) of the entraining cycle.

Constructs of firefly *LUC* reporter gene driven by the *CCA1*, *LHY*, and *TOC1* promoters (Salomé and McClung, 2005) and *LHCB1*1 (CAB2)*:*LUC* in pZP222 vector (−199/+1) (Anderson et al., 1994) were introduced into *skip-1* through transformation.

### Positional Cloning of the *EIP1* Gene

The *eip1-1* mutation was isolated by map-based positional cloning (Lukowitz et al., 2000). To generate a mapping population, *eip1-1* was crossed to Landsberg *erecta* (L*er*), and 467 *eip1-1* plants with early flowering phenotype in the F2 population were scored by PCR for molecular markers cosegregating with the *eip1-1* mutation. The *eip1-1* mutation was initially anchored to the lower arm of chromosome I between AthATPASE and K14-1 simple sequence length polymorphism (see Supplemental Figure 3A online). A high-resolution map was generated using simple sequence length polymorphism or cleaved amplified polymorphic sequences markers by taking advantage of the polymorphism list between Col-0 and L*er* (TAIR; http://www.Arabidopsis.org/). Two recombinants, L12B-57 and L12B-108, flanking a 25-kb region in which there are 13 open reading frames, were obtained between N5-7 and N5-4 cleaved amplified polymorphic sequences markers. The open reading frames in the region were sequenced and a 22-bp deletion was detected in the *SKIP* (At1g77180) locus, which results in a frame shift to truncate the SKIP protein (see Supplemental Figure 3B online).

### Alignment and Molecular Phylogenetic Analysis

Amino acid sequences of At-SKIP and its homologs from other organisms were aligned using Jalview software through ClustalW (Thompson et al., 1994). GenBank accessions of SKIP homologs are the following: *Homo sapiens*, NP_036377, SKIP (Dahl et al., 1998); *Mus musculus*, NP_079783 (Barry et al., 2003); *Drosophila melanogaster*, NP_511093, Bx42 (Saumweber et al., 1990); *Caenorhabditis elegans*, NP_505950 (direct submission); *Oryza sativa japonica*, NP_001048184, Os-SKIP (Tanaka et al., 2008); *Schizosaccharomyces pombe*, NP_588213 (Wood et al., 2002); *Saccharomyces cerevisiae*, NP_00937, Prp45 (Albers et al., 2003); and *Neurospora crassa OR74A*, XP_961188 (Galagan et al., 2003). The corresponding molecular phylogenetic tree was built by maximum likelihood using MEGA 4 (Tamura et al., 2007). The alignment and other parameters used to generate the tree are available as Supplemental Data Set 3 online.

### Complementation Test in *Arabidopsis*

Both genomic and cDNA constructs of *SKIP* were tested for the ability to complement the *skip-1* phenotype. A 5770-bp genomic fragment spanning the *SKIP* locus (2704 bp upstream of the ATG, 1842 bp coding region, and 1201 bp downstream of the TAA) and a *SKIP* cDNA fused to GFP were cloned into the pCambia1300 binary vector. The resulting *SKIP*:*SKIP* and *SKIP*:*GFP-SKIP* plasmids were introduced into *skip-1* by *Agrobacterium tumefaciens*–mediated transformation (Clough and Bent, 1998). Flowering time, leaf movement, and hypocotyl length were determined in the T2 or T3 generations of transgenic lines (*SKIP*:*SKIP/skip-1*). Complemented T3 lines (*SKIP*:*GFP-SKIP/skip-1*) were used for RNA immunoprecipitation (RNA-IP).

### Gene Expression Pattern Assays

*SKIP*:*GUS* transgenic (T3) lines were used to determine the expression pattern of *SKIP* via histochemical GUS reporter activity (Jefferson et al., 1987). Transgenic (T3) lines carrying an N-terminal fusion of GFP to SKIP, driven by the *SKIP* promoter (*SKIP*:*GFP-SKIP*), were generated to determine the tissue, organ, and temporal expression patterns and subcellular localization of SKIP.

For RT-PCR and qRT-PCR, total RNA was extracted from seedlings using TaKaRa RNAiso Plus. After RNase-free DNase I (RQ1 RNase-Free DNase; Promega) treatment, 3 μg of RNA was used for the first-strand cDNA synthesis (RevertAid first-strand cDNA synthesis kit; Fermentas). TaKaRa SYBR Premix Ex Taq and a 7500 Fast Real-Time PCR instrument (Applied Biosystems) were used for qRT-PCR.

For the electropherogram analysis, the forward primers of PRR7 and PRR9 were labeled with carboxyfluorescein. After RT-PCR, the PCR products are applied to ABI3730 sequencer for electrophoresis. Collected data were analyzed with GeneMapper ID v3.2 software.

For RNA gel blot hybridization, 10 μg of total RNA was separated on 1.2% agarose denaturing formaldehyde gels and transferred to nylon membranes. Hybridization probes were radiolabeled and hybridization was done in Church's buffer (Church and Gilbert, 1984) at 65°C overnight with gentle rotation. The blot was washed sequentially with 2× SSC, 1× SSC, and 0.5× SSC, twice each for 10 min at 65°C with gentle rotation. Images were visualized using a phosphor imager (Amersham Biosciences; Storage Phosphor Screen), and the intensities were quantified using ImageQuant software.

### Complementation Analysis in Yeast

The *Bam*HI-*Sal*I fragment of *SKIP* from *Arabidopsis* was cloned under the yeast *ADH1* promoter in pRS416 as *ADH1*:*SKIP*. Rescue of the

morphological defects in *prp45*(1-169) was scored in EGY48 (*MATα ura3-1 leu2-3*, *112 trp1-1 his3-1*, *115 ade2-1 can1-100*), KAY02 [*prp45*(1-169)-*HA*:*kanMX6*] (Siatecka et al., 1999; Gahura et al., 2009), or KAY02 transformed with *ADH1*:*SKIP* plasmid strains and grown at 30 or 37°C on the appropriate selective media for 3 d.

Primer extension was conducted as described previously with slight modification (Siatecka et al., 1999; Gahura et al., 2009). Extension products were separated in an 8% polyacrylamide/8 M urea gel, and the results were visualized by autoradiography.

To determine the band intensity in Figure 5D, we analyzed the band with Quantity One software. The Volume Analysis Report was selected to analyze the band intensity. The mean value in the chosen sizeable box represents the mean intensity of the specific band.

### RNA-IP

The RNA-IP assay was conducted as described previously (Wierzbicki et al., 2008; Zheng et al., 2009) with slight modification. Ten-day-old whole seedlings of transgenic complementation lines harboring *SKIP*:*GFP-SKIP* in the *skip-1* background grown under 12-h-light/12-h-dark conditions were harvested at Zeitgeber time 0 (ZT0) and ZT8 (dawn and 8 h after dawn) to detect the association of SKIP with the pre-mRNA of *PRR7* and *PRR9*. After cross-linking in 1% formaldehyde, a series pre-immunoprecipitation treatment and immunoprecipitation with GFP antibody, the immunoprecipitation products were eluted with immunoprecipitation elution buffer. The associated RNAs were quantified by RT-PCR with primer pairs crossing the intron-exon junctions of *PRR7* and *PRR9* pre-mRNAs after reversing cross-link.

### Confocal Microscopy and FRET Analysis

FRET was conducted as described previously (Más et al., 2000). *35S*:*GFP-SKIP* in pCambia1300 binary vector and *35S*:*SR45-mCherry* or *35S*:*U1-70K-mCherry* in pCambia2300 binary vector were transiently expressed in *Nicotiana benthamiana* leaves infiltrated with *Agrobacterium* strains carrying the appropriate binary plasmids. *pCambia1300-P19* plasmid was coinfiltrated to suppress RNA interference. After 3 d of growth in a greenhouse at 26°C under 16 h light/8 h dark, infiltrated leaves were examined by confocal microscopy.

To test for interaction of SKIP and SR45 or U1-70K, 2- to 3-week-old *N. benthamiana* leaves were transformed with *GFP-SKIP*, *SR45-mCherry*, or *U1-70K-mCherry* alone or with *GFP-SKIP* cotransformed with either *SR45-mCherry* or *U1-70K-mCherry*. Both imaging sensitized emission and acceptor photobleaching approaches for FRET measurement were applied. Three days after transformation, sensitized emission FRET was performed with an Olympus FluoView FV1000 laser scanning confocal microscope. Images in donor (excitation 488 nm; emission 500 to 530 nm), acceptor (excitation 543 nm; emission 560 to 630 nm), and FRET (excitation 488 nm; emission 560 to 630 nm) channels were captured. The energy transfer efficiency and distance between the two interacted proteins were calculated as follows:

$$\text{PFRET} = f\text{-DSBT-ASBT},\ \text{DSBT} = (b/a)\ x\ e,\ \text{ASBT} = (c/d)\ x\ g;\ \text{Efficiency}\ (E)\ =\ 1\text{-}[e/(e{+}\text{PFRET})]$$

where PFRET is precision FRET (correction done FRET image); DSBT is donor spectral bleed-through; ASBT is acceptor spectral bleed-through; *a* is donor channel image of donor excited, with donor only dyed; *b* is acceptor channel image of donor excited, with donor only dyed; *c* is acceptor channel image of donor excited, with acceptor only dyed; *d* is acceptor channel image of acceptor excited, with acceptor only dyed; *e* is donor channel image of donor excited, with donor and acceptor dyed; *f* is acceptor channel image of donor excited, with donor and acceptor dyed; *g* is acceptor channel image of acceptor excited, with donor and acceptor dyed.

For acceptor photobleaching FRET, the fluorescence of the GFP and RFP channels were scanned as for sensitized emission FRET before and after photobleaching. Bleaching of the acceptor fluorescence signal was performed using a 543-nm beam at maximum intensity for 4 s.

### mRNA Sequencing and Bioinformatics Analysis of RNA-Seq Data

For mRNA sequencing, total RNA was isolated using TRI reagent (Ambion). mRNA was extracted from total RNA using Dynabeads mRNA DIRECT kit (Invitrogen). First- and second-strand cDNA was synthesized using Superscript II reverse transcriptase (Invitrogen) and random hexamers primers. DNA Sample Prep Master Mix Set 1 (New England Biolabs) was used to add adapters to the ends of the cDNA. Then, the products of the ligation reaction were purified on a gel to select a size range of templates for downstream enrichment by PCR amplification. After enrichment, the library was sequenced thoroughly.

An overview of the RNA-seq analysis pipeline for reads mapping, expression quantification, detection of differential expression, data visualization, and downstream bioinformatics analysis is summarized in Supplemental Figure 10 online. In brief, the *Arabidopsis* genome build and annotated gene set were downloaded from The Arabidopsis Information Resource (ftp://ftp.Arabidopsis.org/home/tair/Sequences/). After removing reads containing sequencing adapters, we mapped reads to the *Arabidopsis* TAIR9 genome build with BOWTIE (Langmead et al., 2009), allowing up to two mismatches. Reads that failed to be mapped to the genome build were aligned by de novo mapping using BLAT (Kent, 2002) against the same genome build to find splice junctions.

The gene locus expression levels were measured in the reads per kilobase of exon per million mapped reads unit and were calculated based on mapping outputs using ERANGE (Mortazavi et al., 2008). The cutoff value of determining significant expression or translation was 1.0 RPKM based on spike-in controls and reproducibility (Jiao and Meyerowitz, 2010). Differential expression analysis was performed using edgeR using raw mapping counts from BOWTIE and BLAT mapping (Robinson et al., 2010). Data were modeled as negative binomial distributed because our data set contains biological replicates instead of technique replicates. The multiple testing errors were addressed using the false discovery rate. Differential expression cutoff was set as above twofold changes in expression and false discovery rate–adjusted $P < 0.001$. To alleviate the bias in the detection of differential expression influenced by the transcript length (Young et al., 2010), we added the expression ratio cutoff (twofold).

The raw data and processed data of high-throughput mRNA sequencing were submitted to the National Center for Biotechnology Information Gene Expression Omnibus (http://www.ncbi.nlm.nih.gov/geo/query/acc.cgi?acc=GSE32216).

### Novel Splicing Event Detection and Analysis

Splicing events identified by de novo mapping using BLAT were compared with the gene annotation in TAIR9. IR is considered as the complete

retention of an intron in a transcript, which has >1.0 RPKM, the same detection criteria for exons and transcripts (Jiao and Meyerowitz, 2010). Alternative 5′ or 3′SS, ES, or unclassified splicing (with novel 5′ and 3′SSs) is defined by the existence of a de novo mapping identified read, which represents a splicing event not annotated in TAIR9. Alternative splicing events classification is according to Matlin et al. (2005).

Nucleotide frequencies around novel and known splicing sites were counted and visually displayed using sequence logos (Schneider and Stephens, 1990).

### Gene Ontology Analysis

GO analysis was conducted through the website GO Analysis Toolkit and Database for Agricultural Community (Du et al., 2010).

### Accession Numbers

Sequence data from this article can be found in the Arabidopsis Genome Initiative or GenBank/EMBL databases under the following accession numbers: *SKIP* (At1g77180), *PRR7* (At5g02810), *PRR9* (At2g46790), *SR45* (At1g16610), *U1-70K* (At3g50670), *TEJ* (At2g31870), *ARR4* (At1g10470), *CCA1* (At2g46830), *LHY* (At1g01060), *TOC1* (At5g61380), *FIO1* (At2g21070), *ARR3* (At1g59940), *SOC1* (At2g45660), *FT* (At1g65480), *ELF3* (At2g25930), *ELF4* (At2g40080), and *GI* (At1g22770). SKIP homologs are as follows: *H. sapiens*, NP_036377, *M. musculus,* NP_079783, *Drosophila*, NP_511093, *C. elegans*, NP_505950, *O. sativa japonica*, NP_001048184, *S. pombe*, NP_588213, *S. cerevisiae*, NP_00937, and *N. crassa* OR74A, XP_961188.

### Supplemental Data

The following materials are available in the online version of this article.

**Supplemental Figure 1.** Effects of *eip1-1* on Clock Gene Expression in Constant Dark.

**Supplemental Figure 2.** Circadian Expression of *CCA1*, *LHY*, and *TOC1* in the Wild Type and *skip-1*.

**Supplemental Figure 3.** *EIP1* Encodes a Conserved SNW Domain–Containing Protein, SKIP.

**Supplemental Figure 4.** *skip-1* Mutation Does Not Abolish the Expression of *SKIP* Partial Transcript.

**Supplemental Figure 5.** *skip-1* Phenotypes Are Rescued by *SKIP* Genomic DNA.

**Supplemental Figure 6.** Phase Response Curve of *CCA1*:*LUC* Expression to Pulses of Red or Blue Light in the Wild Type and *skip-1*.

**Supplemental Figure 7.** Validation of Intron Retention Splicing Defects in *skip-2* Detected by RNA-Seq through RT-PCR.

**Supplemental Figure 8.** Enriched Gene Ontology Terms (False Detection Rate <0.01) in Genes with Splicing Defects in *skip-2*.

**Supplemental Figure 9.** Expression of *PRR7* and *PRR9* Splicing Isoforms and Splicing Alteration of Circadian Associated and Flowering Time Control Genes in *skip* Detected through RNA Sequencing and RT-PCR.

**Supplemental Figure 10.** The Bioinformatic Pipeline for RNA Sequencing.

**Supplemental Table 1.** Early Flowering and Photoperiod-Insensitive Phenotypes in *eip1-1*.

**Supplemental Table 2.** Circadian Period Lengthening in *eip1-1*/*skip-1* under LL Condition.

**Supplemental Table 3.** *CCA1*:*LUC* Rhythm under Differential Intensity and Spectrum of Light Conditions.

**Supplemental Table 4.** Phase Responses to Red Light and Blue Light Pulses.

**Supplemental Table 5.** Results of Ultra-High-Throughput RNA Sequencing Analysis.

**Supplemental Table 6.** Primers Used in the Studies.

**Supplemental Data Set 1.** Number of New Splicing Events Belonging to Four Alternative Splicing Types in *skip-2*.

**Supplemental Data Set 2.** The Frequency Distribution of Nucleotides at 5 and 3 Prime Splicing Site.

**Supplemental Data Set 3.** Text File of the Alignment Used to Generate the Phylogenetic Tree Shown in Supplemental Figure 3C.

## ACKNOWLEDGMENTS

We thank Petr Folk for critical reading of the article, Chen Zhan and Ping Wu for their technical assistance with FRET and GFP fluorescence, Yuelin Zhang for his suggestion on positional cloning, Lilin Du for the pRS416 plasmid, and Zhiyu Peng for his help on RNA-seq analysis. We acknowledge the Arabidopsis Genome Initiative and the ABRC for providing us with the polymorphism between *Arabidopsis* Col-0 and L*er* ecotypes and the T-DNA insertion line, respectively. This work was supported by grants from Ministry of Science and Technology of China 973 projects (2012CB910900 and 2012CB114200; L.M.), by the Hebei Province key laboratory program (L.M.), by the National Science Foundation of China (X.X. and Y.C.), and by the National Science Foundation (IOS-0950703 and IOS1025965; C.R.M.).

## AUTHOR CONTRIBUTIONS

L.M., X.X, X.W., Q.X., F.W., Y.C., and C.R.M. designed the study. X.W. and H.W. identified the mutant, cloned the gene, provided the *SKIP*-related constructs, and generated all the transgenic lines. X.X., Q.X., and X.W. performed circadian clock analysis. F.W. and L.L. performed FRET. F.W. performed RIP experiments. F.W., O.G., and F.P. performed yeast complementation and primer extension assay. X.W., Y.Y., and F.W. performed oscillator gene pre-mRNA splicing assay. Y.W., Y.J., X.W., and S.M. performed the RNA-seq analysis and validation. L.M., X.X., C.R.M., X.W., Q.X., and F.W. wrote the article. All authors discussed the results and commented on the article.

Received April 30, 2012; revised June 15, 2012; accepted August 1, 2012; published August 31, 2012.

## REFERENCES

**Albers, M., Diment, A., Muraru, M., Russell, C.S., and Beggs, J.D.** (2003). Identification and characterization of Prp45p and Prp46p, essential pre-mRNA splicing factors. RNA **9:** 138–150.

**Ali, G.S., Palusa, S.G., Golovkin, M., Prasad, J., Manley, J.L., and Reddy, A.S.** (2007). Regulation of plant developmental processes by a novel splicing factor. PLoS ONE **2:** e471.

**Anderson, S.L., Teakle, G.R., Martino-Catt, S.J., and Kay, S.A.** (1994). Circadian clock- and phytochrome-regulated transcription is conferred by a 78 bp cis-acting domain of the Arabidopsis CAB2 promoter. Plant J. **6:** 457–470.

**Aschoff, J.** (1979). Circadian rhythms: Influences of internal and external factors on the period measured in constant conditions. Z. Tierpsychol. **49:** 225–249.

**Barry, J.B., Leong, G.M., Church, W.B., Issa, L.L., Eisman, J.A., and Gardiner, E.M.** (2003). Interactions of SKIP/NCoA-62, TFIIB, and

retinoid X receptor with vitamin D receptor helix H10 residues. J. Biol. Chem. **278:** 8224–8228.

**Behzadnia, N., Golas, M.M., Hartmuth, K., Sander, B., Kastner, B., Deckert, J., Dube, P., Will, C.L., Urlaub, H., Stark, H., and Lührmann, R.** (2007). Composition and three-dimensional EM structure of double affinity-purified, human prespliceosomal A complexes. EMBO J. **26:** 1737–1748.

**Bell-Pedersen, D., Cassone, V.M., Earnest, D.J., Golden, S.S., Hardin, P.E., Thomas, T.L., and Zoran, M.J.** (2005). Circadian rhythms from multiple oscillators: Lessons from diverse organisms. Nat. Rev. Genet. **6:** 544–556.

**Bessonov, S., Anokhina, M., Will, C.L., Urlaub, H., and Lührmann, R.** (2008). Isolation of an active step I spliceosome and composition of its RNP core. Nature **452:** 846–850.

**Brès, V., Gomes, N., Pickle, L., and Jones, K.A.** (2005). A human splicing factor, SKIP, associates with P-TEFb and enhances transcription elongation by HIV-1 Tat. Genes Dev. **19:** 1211–1226.

**Brès, V., Yoshida, T., Pickle, L., and Jones, K.A.** (2009). SKIP interacts with c-Myc and Menin to promote HIV-1 Tat transactivation. Mol. Cell **36:** 75–87.

**Chen, Y., Zhang, L., and Jones, K.A.** (2011). SKIP counteracts p53-mediated apoptosis via selective regulation of p21Cip1 mRNA splicing. Genes Dev. **25:** 701–716.

**Cheng, Y., Gvakharia, B., and Hardin, P.E.** (1998). Two alternatively spliced transcripts from the Drosophila period gene rescue rhythms having different molecular and behavioral characteristics. Mol. Cell. Biol. **18:** 6505–6514.

**Chow, B.Y., Helfer, A., Nusinow, D.A., and Kay, S.A.** (2012). ELF3 recruitment to the *PRR9* promoter requires other Evening Complex members in the Arabidopsis circadian clock. Plant Signal. Behav. **7:** 170–173.

**Church, G.M., and Gilbert, W.** (1984). Genomic sequencing. Proc. Natl. Acad. Sci. USA **81:** 1991–1995.

**Clough, S.J., and Bent, A.F.** (1998). Floral dip: A simplified method for Agrobacterium-mediated transformation of *Arabidopsis thaliana*. Plant J. **16:** 735–743.

**Colot, H.V., Loros, J.J., and Dunlap, J.C.** (2005). Temperature-modulated alternative splicing and promoter use in the Circadian clock gene frequency. Mol. Biol. Cell **16:** 5563–5571.

**Dahl, R., Wani, B., and Hayman, M.J.** (1998). The Ski oncoprotein interacts with Skip, the human homolog of Drosophila Bx42. Oncogene **16:** 1579–1586.

**Daniel, X., Sugano, S., and Tobin, E.M.** (2004). CK2 phosphorylation of CCA1 is necessary for its circadian oscillator function in Arabidopsis. Proc. Natl. Acad. Sci. USA **101:** 3292–3297.

**Deckert, J., Hartmuth, K., Boehringer, D., Behzadnia, N., Will, C.L., Kastner, B., Stark, H., Urlaub, H., and Lührmann, R.** (2006). Protein composition and electron microscopy structure of affinity-purified human spliceosomal B complexes isolated under physiological conditions. Mol. Cell. Biol. **26:** 5528–5543.

**Deng, X., Gu, L., Liu, C., Lu, T., Lu, F., Lu, Z., Cui, P., Pei, Y., Wang, B., Hu, S., and Cao, X.** (2010). Arginine methylation mediated by the Arabidopsis homolog of PRMT5 is essential for proper pre-mRNA splicing. Proc. Natl. Acad. Sci. USA **107:** 19114–19119.

**Dinesh-Kumar, S.P., and Baker, B.J.** (2000). Alternatively spliced N resistance gene transcripts: Their possible role in tobacco mosaic virus resistance. Proc. Natl. Acad. Sci. USA **97:** 1908–1913.

**Ding, Z., Millar, A.J., Davis, A.M., and Davis, S.J.** (2007). TIME FOR COFFEE encodes a nuclear regulator in the *Arabidopsis thaliana* circadian clock. Plant Cell **19:** 1522–1536.

**Du, Z., Zhou, X., Ling, Y., Zhang, Z., and Su, Z.** (2010). agriGO: A GO analysis toolkit for the agricultural community. Nucleic Acids Res. **38**(Web Server issue)**:** W64–W70.

**Farinas, B., and Mas, P.** (2011). Functional implication of the MYB transcription factor RVE8/LCL5 in the circadian control of histone acetylation. Plant J. **66:** 318–329.

**Farré, E.M., Harmer, S.L., Harmon, F.G., Yanovsky, M.J., and Kay, S.A.** (2005). Overlapping and distinct roles of PRR7 and PRR9 in the Arabidopsis circadian clock. Curr. Biol. **15:** 47–54.

**Figueroa, J.D., and Hayman, M.J.** (2004). The human Ski-interacting protein functionally substitutes for the yeast PRP45 gene. Biochem. Biophys. Res. Commun. **319:** 1105–1109.

**Filichkin, S.A., Priest, H.D., Givan, S.A., Shen, R., Bryant, D.W., Fox, S.E., Wong, W.K., and Mockler, T.C.** (2010). Genome-wide mapping of alternative splicing in *Arabidopsis thaliana*. Genome Res. **20:** 45–58.

**Fujiwara, S., Wang, L., Han, L., Suh, S.S., Salomé, P.A., McClung, C.R., and Somers, D.E.** (2008). Post-translational regulation of the Arabidopsis circadian clock through selective proteolysis and phosphorylation of pseudo-response regulator proteins. J. Biol. Chem. **283:** 23073–23083.

**Gahura, O., Abrhámová, K., Skruzný, M., Valentová, A., Munzarová, V., Folk, P., and Půta, F.** (2009). Prp45 affects Prp22 partition in spliceosomal complexes and splicing efficiency of non-consensus substrates. J. Cell. Biochem. **106:** 139–151.

**Galagan, J.E., et al**. (2003). The genome sequence of the filamentous fungus *Neurospora crassa*. Nature **422:** 859–868.

**Gendron, J.M., Pruneda-Paz, J.L., Doherty, C.J., Gross, A.M., Kang, S.E., and Kay, S.A.** (2012). Arabidopsis circadian clock protein, TOC1, is a DNA-binding transcription factor. Proc. Natl. Acad. Sci. USA **109:** 3167–3172.

**Golovkin, M., and Reddy, A.S.** (1996). Structure and expression of a plant U1 snRNP 70K gene: Alternative splicing of U1 snRNP 70K pre-mRNAs produces two different transcripts. Plant Cell **8:** 1421–1435.

**Gould, P.D., Locke, J.C., Larue, C., Southern, M.M., Davis, S.J., Hanano, S., Moyle, R., Milich, R., Putterill, J., Millar, A.J., and Hall, A.** (2006). The molecular basis of temperature compensation in the *Arabidopsis* circadian clock. Plant Cell **18:** 1177–1187.

**Guo, J., Cheng, P., Yuan, H., and Liu, Y.** (2009). The exosome regulates circadian gene expression in a posttranscriptional negative feedback loop. Cell **138:** 1236–1246.

**Hall, A., Bastow, R.M., Davis, S.J., Hanano, S., McWatters, H.G., Hibberd, V., Doyle, M.R., Sung, S., Halliday, K.J., Amasino, R.M., and Millar, A.J.** (2003). The TIME FOR COFFEE gene maintains the amplitude and timing of *Arabidopsis* circadian clocks. Plant Cell **15:** 2719–2729.

**Harmer, S.** (2010). Plant biology in the fourth dimension. Plant Physiol. **154:** 467–470.

**Harmer, S.L.** (2009). The circadian system in higher plants. Annu. Rev. Plant Biol. **60:** 357–377.

**Harms, E., Kivimäe, S., Young, M.W., and Saez, L.** (2004). Post-transcriptional and posttranslational regulation of clock genes. J. Biol. Rhythms **19:** 361–373.

**Hazen, S.P., Naef, F., Quisel, T., Gendron, J.M., Chen, H., Ecker, J.R., Borevitz, J.O., and Kay, S.A.** (2009). Exploring the transcriptional landscape of plant circadian rhythms using genome tiling arrays. Genome Biol. **10:** R17.

**Hazen, S.P., Schultz, T.F., Pruneda-Paz, J.L., Borevitz, J.O., Ecker, J.R., and Kay, S.A.** (2005). LUX ARRHYTHMO encodes a Myb domain protein essential for circadian rhythms. Proc. Natl. Acad. Sci. USA **102:** 10387–10392.

**Helfer, A., Nusinow, D.A., Chow, B.Y., Gehrke, A.R., Bulyk, M.L., and Kay, S.A.** (2011). LUX ARRHYTHMO encodes a nighttime repressor of circadian gene expression in the Arabidopsis core clock. Curr. Biol. **21:** 126–133.

**Hong, S., Song, H.R., Lutz, K., Kerstetter, R.A., Michael, T.P., and McClung, C.R.** (2010). Type II protein arginine methyltransferase 5

(PRMT5) is required for circadian period determination in *Arabidopsis thaliana*. Proc. Natl. Acad. Sci. USA **107:** 21211–21216.

**Hou, X., Xie, K., Yao, J., Qi, Z., and Xiong, L.** (2009). A homolog of human ski-interacting protein in rice positively regulates cell viability and stress tolerance. Proc. Natl. Acad. Sci. USA **106:** 6410–6415.

**Huang, W., Pérez-García, P., Pokhilko, A., Millar, A.J., Antoshechkin, I., Riechmann, J.L., and Mas, P.** (2012). Mapping the core of the Arabidopsis circadian clock defines the network structure of the oscillator. Science **336:** 75–79.

**James, A.B., Syed, N.H., Bordage, S., Marshall, J., Nimmo, G.A., Jenkins, G.I., Herzyk, P., Brown, J.W., and Nimmo, H.G.** (2012). Alternative splicing mediates responses of the *Arabidopsis* circadian clock to temperature changes. Plant Cell **24:** 961–981.

**Jefferson, R.A., Kavanagh, T.A., and Bevan, M.W.** (1987). GUS fusions: Beta-glucuronidase as a sensitive and versatile gene fusion marker in higher plants. EMBO J. **6:** 3901–3907.

**Jiao, Y., and Meyerowitz, E.M.** (2010). Cell-type specific analysis of translating RNAs in developing flowers reveals new levels of control. Mol. Syst. Biol. **6:** 419.

**Johnson, C.H.** (1999). Forty years of PRCs—What have we learned? Chronobiol. Int. **16:** 711–743.

**Jordan, T., Schornack, S., and Lahaye, T.** (2002). Alternative splicing of transcripts encoding Toll-like plant resistance proteins - What's the functional relevance to innate immunity? Trends Plant Sci. **7:** 392–398.

**Kent, W.J.** (2002). BLAT—The BLAST-like alignment tool. Genome Res. **12:** 656–664.

**Kiba, T., Henriques, R., Sakakibara, H., and Chua, N.H.** (2007). Targeted degradation of PSEUDO-RESPONSE REGULATOR5 by an SCFZTL complex regulates clock function and photomorphogenesis in *Arabidopsis thaliana*. Plant Cell **19:** 2516–2530.

**Kim, W.Y., Fujiwara, S., Suh, S.S., Kim, J., Kim, Y., Han, L., David, K., Putterill, J., Nam, H.G., and Somers, D.E.** (2007). ZEITLUPE is a circadian photoreceptor stabilized by GIGANTEA in blue light. Nature **449:** 356–360.

**Kim, W.Y., Salomé, P.A., Fujiwara, S., Somers, D.E., and McClung, C.R.** (2010). Characterization of pseudo-response regulators in plants. Methods Enzymol. **471:** 357–378.

**Koornneef, M., Hanhart, C.J., and van der Veen, J.H.** (1991). A genetic and physiological analysis of late flowering mutants in *Arabidopsis thaliana*. Mol. Gen. Genet. **229:** 57–66.

**Langmead, B., Trapnell, C., Pop, M., and Salzberg, S.L.** (2009). Ultrafast and memory-efficient alignment of short DNA sequences to the human genome. Genome Biol. **10:** R25.

**Lim, G.H., Zhang, X., Chung, M.S., Lee, D.J., Woo, Y.M., Cheong, H.S., and Kim, C.S.** (2010). A putative novel transcription factor, AtSKIP, is involved in abscisic acid signalling and confers salt and osmotic tolerance in Arabidopsis. New Phytol. **185:** 103–113.

**Locke, J.C., Southern, M.M., Kozma-Bognar, L., Hibberd, V., Brown, P.E., Turner, M.S., and Millar, A.J.** (2005). Extension of a genetic network model by iterative experimentation and mathematical analysis. Mol. Syst. Biol. **1:** 2005.0013.

**Lorković, Z.J., Wieczorek Kirk, D.A., Lambermon, M.H., and Filipowicz, W.** (2000). Pre-mRNA splicing in higher plants. Trends Plant Sci. **5:** 160–167.

**Lukowitz, W., Gillmor, C.S., and Scheible, W.R.** (2000). Positional cloning in Arabidopsis. Why it feels good to have a genome initiative working for you. Plant Physiol. **123:** 795–805.

**Macknight, R., Duroux, M., Laurie, R., Dijkwel, P., Simpson, G., and Dean, C.** (2002). Functional significance of the alternative transcript processing of the *Arabidopsis* floral promoter FCA. Plant Cell **14:** 877–888.

**Martin-Tryon, E.L., and Harmer, S.L.** (2008). XAP5 CIRCADIAN TIMEKEEPER coordinates light signals for proper timing of photomorphogenesis and the circadian clock in *Arabidopsis*. Plant Cell **20:** 1244–1259.

**Más, P., Devlin, P.F., Panda, S., and Kay, S.A.** (2000). Functional interaction of phytochrome B and cryptochrome 2. Nature **408:** 207–211.

**Más, P., Kim, W.Y., Somers, D.E., and Kay, S.A.** (2003). Targeted degradation of TOC1 by ZTL modulates circadian function in *Arabidopsis thaliana*. Nature **426:** 567–570.

**Más, P., and Yanovsky, M.J.** (2009). Time for circadian rhythms: Plants get synchronized. Curr. Opin. Plant Biol. **12:** 574–579.

**Matlin, A.J., Clark, F., and Smith, C.W.** (2005). Understanding alternative splicing: Towards a cellular code. Nat. Rev. Mol. Cell Biol. **6:** 386–398.

**McClung, C.R.** (2006). Plant circadian rhythms. Plant Cell **18:** 792–803.

**McClung, C.R., and Gutiérrez, R.A.** (2010). Network news: Prime time for systems biology of the plant circadian clock. Curr. Opin. Genet. Dev. **20:** 588–598.

**Mehra, A., Baker, C.L., Loros, J.J., and Dunlap, J.C.** (2009). Post-translational modifications in circadian rhythms. Trends Biochem. Sci. **34:** 483–490.

**Michael, T.P., Salomé, P.A., Yu, H.J., Spencer, T.R., Sharp, E.L., McPeek, M.A., Alonso, J.M., Ecker, J.R., and McClung, C.R.** (2003). Enhanced fitness conferred by naturally occurring variation in the circadian clock. Science **302:** 1049–1053.

**Millar, A.J., Straume, M., Chory, J., Chua, N.H., and Kay, S.A.** (1995). The regulation of circadian period by phototransduction pathways in Arabidopsis. Science **267:** 1163–1166.

**Mizoguchi, T., Wright, L., Fujiwara, S., Cremer, F., Lee, K., Onouchi, H., Mouradov, A., Fowler, S., Kamada, H., Putterill, J., and Coupland, G.** (2005). Distinct roles of GIGANTEA in promoting flowering and regulating circadian rhythms in *Arabidopsis*. Plant Cell **17:** 2255–2270.

**Moore, M.J., and Proudfoot, N.J.** (2009). Pre-mRNA processing reaches back to transcription and ahead to translation. Cell **136:** 688–700.

**Mortazavi, A., Williams, B.A., McCue, K., Schaeffer, L., and Wold, B.** (2008). Mapping and quantifying mammalian transcriptomes by RNA-Seq. Nat. Methods **5:** 621–628.

**Nagoshi, E., Saini, C., Bauer, C., Laroche, T., Naef, F., and Schibler, U.** (2004). Circadian gene expression in individual fibroblasts: Cell-autonomous and self-sustained oscillators pass time to daughter cells. Cell **119:** 693–705.

**Nakamichi, N., Kiba, T., Henriques, R., Mizuno, T., Chua, N.H., and Sakakibara, H.** (2010). PSEUDO-RESPONSE REGULATORS 9, 7, and 5 are transcriptional repressors in the *Arabidopsis* circadian clock. Plant Cell **22:** 594–605.

**Nusinow, D.A., Helfer, A., Hamilton, E.E., King, J.J., Imaizumi, T., Schultz, T.F., Farré, E.M., and Kay, S.A.** (2011). The ELF4-ELF3-LUX complex links the circadian clock to diurnal control of hypocotyl growth. Nature **475:** 398–402.

**Onai, K., and Ishiura, M.** (2005). PHYTOCLOCK 1 encoding a novel GARP protein essential for the Arabidopsis circadian clock. Genes Cells **10:** 963–972.

**Para, A., Farré, E.M., Imaizumi, T., Pruneda-Paz, J.L., Harmon, F.G., and Kay, S.A.** (2007). PRR3 is a vascular regulator of TOC1 stability in the *Arabidopsis* circadian clock. Plant Cell **19:** 3462–3473.

**Park, D.H., Somers, D.E., Kim, Y.S., Choy, Y.H., Lim, H.K., Soh, M.S., Kim, H.J., Kay, S.A., and Nam, H.G.** (1999). Control of circadian rhythms and photoperiodic flowering by the Arabidopsis GIGANTEA gene. Science **285:** 1579–1582.

**Plautz, J.D., Straume, M., Stanewsky, R., Jamison, C.F., Brandes, C., Dowse, H.B., Hall, J.C., and Kay, S.A.** (1997). Quantitative analysis of Drosophila period gene transcription in living animals. J. Biol. Rhythms **12:** 204–217.

**Pokhilko, A., Fernández, A.P., Edwards, K.D., Southern, M.M., Halliday, K.J., and Millar, A.J.** (2012). The clock gene circuit in Arabidopsis includes a repressilator with additional feedback loops. Mol. Syst. Biol. **8:** 574.

**Pruneda-Paz, J.L., and Kay, S.A.** (2010). An expanding universe of circadian networks in higher plants. Trends Plant Sci. **15:** 259–265.

**Quesada, V., Macknight, R., Dean, C., and Simpson, G.G.** (2003). Autoregulation of FCA pre-mRNA processing controls Arabidopsis flowering time. EMBO J. **22:** 3142–3152.

**Rawat, R., Takahashi, N., Hsu, P.Y., Jones, M.A., Schwartz, J., Salemi, M.R., Phinney, B.S., and Harmer, S.L.** (2011). REVEILLE8 and PSEUDO-REPONSE REGULATOR5 form a negative feedback loop within the Arabidopsis circadian clock. PLoS Genet. **7:** e1001350.

**Reddy, A.S.** (2007). Alternative splicing of pre-messenger RNAs in plants in the genomic era. Annu. Rev. Plant Biol. **58:** 267–294.

**Rédei, G.P.** (1962). Supervital mutants of Arabidopsis. Genetics **47:** 443–460.

**Robinson, M.D., McCarthy, D.J., and Smyth, G.K.** (2010). edgeR: A Bioconductor package for differential expression analysis of digital gene expression data. Bioinformatics **26:** 139–140.

**Salomé, P.A., and McClung, C.R.** (2005). PSEUDO-RESPONSE REGULATOR 7 and 9 are partially redundant genes essential for the temperature responsiveness of the *Arabidopsis* circadian clock. Plant Cell **17:** 791–803.

**Salomé, P.A., Weigel, D., and McClung, C.R.** (2010). The role of the *Arabidopsis* morning loop components CCA1, LHY, PRR7, and PRR9 in temperature compensation. Plant Cell **22:** 3650–3661.

**Sanchez, S.E., et al**. (2010). A methyl transferase links the circadian clock to the regulation of alternative splicing. Nature **468:** 112–116.

**Saumweber, H., Frasch, M., and Korge, G.** (1990). Two puff-specific proteins bind within the 2.5 kb upstream region of the Drosophila melanogaster Sgs-4 gene. Chromosoma **99:** 52–60.

**Schneider, T.D., and Stephens, R.M.** (1990). Sequence logos: A new way to display consensus sequences. Nucleic Acids Res. **18:** 6097–6100.

**Scott, K.L., and Plon, S.E.** (2005). CHES1/FOXN3 interacts with Ski-interacting protein and acts as a transcriptional repressor. Gene **359:** 119–126.

**Siatecka, M., Reyes, J.L., and Konarska, M.M.** (1999). Functional interactions of Prp8 with both splice sites at the spliceosomal catalytic center. Genes Dev. **13:** 1983–1993.

**Somers, D.E., Devlin, P.F., and Kay, S.A.** (1998). Phytochromes and cryptochromes in the entrainment of the Arabidopsis circadian clock. Science **282:** 1488–1490.

**Southern, M.M., and Millar, A.J.** (2005). Circadian genetics in the model higher plant, *Arabidopsis thaliana*. Methods Enzymol. **393:** 23–35.

**Sugano, S., Andronis, C., Green, R.M., Wang, Z.Y., and Tobin, E.M.** (1998). Protein kinase CK2 interacts with and phosphorylates the Arabidopsis circadian clock-associated 1 protein. Proc. Natl. Acad. Sci. USA **95:** 11020–11025.

**Tamura, K., Dudley, J., Nei, M., and Kumar, S.** (2007). MEGA4: Molecular Evolutionary Genetics Analysis (MEGA) software version 4.0. Mol. Biol. Evol. **24:** 1596–1599.

**Tanabe, N., Kimura, A., Yoshimura, K., and Shigeoka, S.** (2009). Plant-specific SR-related protein atSR45a interacts with spliceosomal proteins in plant nucleus. Plant Mol. Biol. **70:** 241–252.

**Tanaka, T., et al; Rice Annotation Project** (2008). The Rice Annotation Project Database (RAP-DB): 2008 update. Nucleic Acids Res. **36**(Database issue)**:** D1028–D1033.

**Thompson, J.D., Higgins, D.G., and Gibson, T.J.** (1994). CLUSTAL W: Improving the sensitivity of progressive multiple sequence alignment through sequence weighting, position-specific gap penalties and weight matrix choice. Nucleic Acids Res. **22:** 4673–4680.

**Tseng, T.S., Salomé, P.A., McClung, C.R., and Olszewski, N.E.** (2004). SPINDLY and GIGANTEA interact and act in *Arabidopsis thaliana* pathways involved in light responses, flowering, and rhythms in cotyledon movements. Plant Cell **16:** 1550–1563.

**Wahl, M.C., Will, C.L., and Lührmann, R.** (2009). The spliceosome: Design principles of a dynamic RNP machine. Cell **136:** 701–718.

**Wang, L., Fujiwara, S., and Somers, D.E.** (2010). PRR5 regulates phosphorylation, nuclear import and subnuclear localization of TOC1 in the Arabidopsis circadian clock. EMBO J. **29:** 1903–1915.

**Wierzbicki, A.T., Haag, J.R., and Pikaard, C.S.** (2008). Noncoding transcription by RNA polymerase Pol IVb/Pol V mediates transcriptional silencing of overlapping and adjacent genes. Cell **135:** 635–648.

**Wijnen, H., and Young, M.W.** (2006). Interplay of circadian clocks and metabolic rhythms. Annu. Rev. Genet. **40:** 409–448.

**Wood, V., et al**. (2002). The genome sequence of *Schizosaccharomyces pombe*. Nature **415:** 871–880. Erratum. Nature **421:** 94.

**Young, M.D., Wakefield, M.J., Smyth, G.K., and Oshlack, A.** (2010). Gene ontology analysis for RNA-seq: Accounting for selection bias. Genome Biol. **11:** R14.

**Zagotta, M.T., Hicks, K.A., Jacobs, C.I., Young, J.C., Hangarter, R.P., and Meeks-Wagner, D.R.** (1996). The Arabidopsis ELF3 gene regulates vegetative photomorphogenesis and the photoperiodic induction of flowering. Plant J. **10:** 691–702.

**Zhang, C., Dowd, D.R., Staal, A., Gu, C., Lian, J.B., van Wijnen, A.J., Stein, G.S., and MacDonald, P.N.** (2003). Nuclear coactivator-62 kDa/Ski-interacting protein is a nuclear matrix-associated coactivator that may couple vitamin D receptor-mediated transcription and RNA splicing. J. Biol. Chem. **278:** 35325–35336.

**Zhang, E.E., and Kay, S.A.** (2010). Clocks not winding down: Unravelling circadian networks. Nat. Rev. Mol. Cell Biol. **11:** 764–776.

**Zhang, X.N., and Mount, S.M.** (2009). Two alternatively spliced isoforms of the Arabidopsis SR45 protein have distinct roles during normal plant development. Plant Physiol. **150:** 1450–1458.

**Zheng, B., Wang, Z., Li, S., Yu, B., Liu, J.Y., and Chen, X.** (2009). Intergenic transcription by RNA polymerase II coordinates Pol IV and Pol V in siRNA-directed transcriptional gene silencing in Arabidopsis. Genes Dev. **23:** 2850–2860.

**Zimmerman, W.F., Pittendrigh, C.S., and Pavlidis, T.** (1968). Temperature compensation of the circadian oscillation in *Drosophila pseudoobscura* and its entrainment by temperature cycles. J. Insect Physiol. **14:** 669–684.